

DETERMINATION OF THE DIURNAL VARIATION OF
EDDY CONDUCTIVITY NEAR THE EARTH'S SURFACE

BY
BENJAMIN CLARK COOLEY

Thesis
C748

THESIS
C748

Library
U. S. Naval Postgraduate School
Annapolis, Md.



DETERMINATION OF THE DIURNAL VARIATION OF
EDDY CONDUCTIVITY NEAR THE EARTH'S SURFACE

by
B. C. Cooley

Thesis
C748

DETERMINATION OF THE DIURNAL VARIATION OF
EDDY CONDUCTIVITY NEAR THE EARTH'S SURFACE

by
Benjamin Clark Cooley
Lieutenant Commander, United States Navy

Submitted in partial fulfillment
of the requirements
for the degree of
MASTER OF SCIENCE
IN AERROLOGY

United States Naval Postgraduate School
Monterey, California
1950

This work is accepted as fulfilling
the thesis requirements for the degree of

MASTER OF SCIENCE
IN AEROLOGY

from the
United States Naval Postgraduate School

PREFACE

The object of this study is to determine the coefficient of eddy conduction, its variation with height, and its diurnal variation in the surface layer.

This paper was prepared at the U. S. Naval Postgraduate School, Monterey, California during the period December 1949 to May 1950.

The author expresses his appreciation and thanks to Associate Professor Frank L. Martin, who gave valuable advice and guidance in the development of this paper.

TABLE OF CONTENTS

	Page
CERTIFICATE OF APPROVAL	i
PREFACE	ii
TABLE OF CONTENTS	iii
LIST OF ILLUSTRATIONS	iv
TABLE OF SYMBOLS AND ABBREVIATIONS	v
CHAPTER	
I. INTRODUCTION	1
II. THE NATURE OF THE DATA	4
1. The Data	4
2. Selection of Data for This Study	4
III. THEORETICAL AND EMPIRICAL CONCEPTS	6
1. The Water Vapor Radiative Transfer Problem	6
2. The Carbon Dioxide Radiative Transfer Problem	7
3. Heat Transfer by Molecular Conductivity	11
4. Rate of Change of Temperature by Eddy Conductivity	12
5. The Coefficient of Eddy Conduction	12
IV. RATES OF CHANGE OF TEMPERATURE	16
1. Rate of Change of Temperature Due to Water Vapor	16
2. Rate of Change of Temperature Due to Carbon Dioxide	22
3. Resultant Radiative Rate of Temperature Change	25
4. Rate of Change of Temperature Due to Molecular Conduction	27
5. Rate of Change of Temperature Due to Eddy Conduction	27
V. RESULTS AND CONCLUSIONS	29
1. Method of Computation of the Coefficient of Eddy Conduction	29
2. Discussion of Results	41
BIBLIOGRAPHY	47

LIST OF ILLUSTRATIONS

	Page
Tables	
1. Heat Transfer Due to Water Vapor, cal (3 hr) ⁻¹	20
2. Three-hourly Rate of Change of Temperature Due to Water Vapor	21
3. Heat Transfer Due to Carbon Dioxide, cal (3 hr) ⁻¹	23
4. Three-hourly Rate of Temperature-Change Due to Carbon Dioxide	24
5. Half-hourly Rate of Temperature-change: Water Vapor Carbon Dioxide	26
6. Half-hourly Rate of Temperature-change Due to Eddy Conduction	27
7. Half-hourly Temperature-change Due to Eddy Conduction	28
8. Computation Values for Determination of K at Reference Level	32
9. The Coefficient of Eddy Conduction, K, (cm ² sec ⁻¹)	34
10. Values of Lapse Rates at 0200 and 1300 LCT	42
11. Slopes of Log K against Log Z for the Lines of Plate I	44
Figures	
1. Difference of Net Fluxes for a Slab Below 288 Feet (Typical Night-time Conditions)	17
2. Difference of Net Fluxes for a Slab Below 288 Feet (Typical Day-time Conditions)	18
3. Adiabatic Velocity Profile (A.M. - P.M. Average)	31
4. Diurnal Variation of K at .25 Feet	36
5. Diurnal Variation of K at 6 Feet	37
6. Diurnal Variation of K at 30 Feet	38
7. Diurnal Variation of K at 60 Feet	39
8. Diurnal Variation of K at 125 Feet	40

PLATE (inside back cover)

I Variation of K with Height

TABLE OF SYMBOLS AND ABBREVIATIONS

A	percentage energy absorbed by a thickness, c, of carbon dioxide
c	the equivalent thickness of carbon dioxide in cms
c_p	specific heat of air in gm cal
E	flux in the band 13.3 - 17.1 microns entering the second boundary of a slab
E_{λ_0}	flux in the band 13.3 - 17.1 microns entering the first boundary of a slab
E_{λ_1}	black body flux in the band 13.3 - 17.1 microns for the mean temperature of the slab
F_1	net upward flux at bottom of the slab
F_2	net upward flux at top of the slab
F_m	upward flux of heat due to molecular conduction
g	acceleration of gravity
K	coefficient of eddy conduction
k	Von Karman constant ($k = .45$)
l	mixing length in a non-isotropic atmosphere
l_a	mixing length in an isotropic atmosphere
m	slope of the curve log K against log Z
n, x	coefficients given by Callendar for computing monochromatic absorptivity in the carbon dioxide band 13.0 - 17.0 microns
p	atmospheric pressure in millibars
p_a	atmospheric pressure in atmospheres
p_i	mean pressure of the i-th slab
q_i	mean specific humidity of the i-th slab
R_d	gas constant per gram of dry air
T	absolute temperature
T_m	mean absolute temperature

u	horizontal wind speed
u_a	horizontal wind speed in an isotropic atmosphere
Z	height measured from the base of the tower
α	coefficient of molecular conduction
γ	the existing lapse rate
γ_d	dry adiabatic lapse rate
θ	potential temperature
τ	constant stress in the surface layer
τ_a	constant stress in the surface layer of an isotropic atmosphere

I. INTRODUCTION

During 1948-1949 several articles have been published by the University of Texas giving half-hourly observations of both temperature and wind at various levels from the ground up to and including 288 feet for periods of approximately one day. This suggested the problem of determining the coefficient of eddy conductivity using the observed lapse rate data; and, the coefficient of viscosity by using the observed wind profile data. These two coefficients were found, in 1936, by Sverdrup [11] to be equal in the atmosphere, but other eddy diffusion coefficients were found by him to be unequal. On the other hand, Petterssen and Swinbank [10], in 1947, suggest that the former coefficient is more nearly related to the latter by the factor .65 in the free atmosphere. The question appears to require another critical examination; and, with the availability of new and fairly accurate data, it seemed to be a problem well worthy of study. In actuality, the problem of determining the diurnal variation of the coefficient of eddy conductivity, K , near the ground proved to be so complex that this was all that time permitted in this dissertation. It will be necessary to answer the question of the equality of the two coefficients at some later date. However, the determination of values of the coefficient of eddy conductivity and its diurnal variation, determined purely from heat transfer considerations, is of some practical interest as a check on previously determined values. For example, Stewart [1] indicates a possible range of $10^3 \text{ cm}^2 \text{ sec}^{-1}$ to $10^5 \text{ cm}^2 \text{ sec}^{-1}$ for K within the surface layer, depending upon the stability of the layer.

THE HISTORY OF THE

THE HISTORY OF THE

THE HISTORY OF THE

THE HISTORY OF THE

THE HISTORY OF THE

THE HISTORY OF THE

THE HISTORY OF THE

THE HISTORY OF THE

THE HISTORY OF THE

THE HISTORY OF THE

THE HISTORY OF THE

THE HISTORY OF THE

THE HISTORY OF THE

THE HISTORY OF THE

THE HISTORY OF THE

THE HISTORY OF THE

THE HISTORY OF THE

THE HISTORY OF THE

THE HISTORY OF THE

THE HISTORY OF THE

THE HISTORY OF THE

THE HISTORY OF THE

THE HISTORY OF THE

THE HISTORY OF THE

This study gives explicit values of K , with respect to local civil time, corresponding to a particular synoptic situation, that for the period 27-28 September 1948 in the vicinity of Manor, Texas. Another important result of this study proved to be the determination of rates of radiative heating and cooling of the layers of air near the ground at various times covering a full day. This yielded some surprisingly large values. These results could be used to solve a problem proposed by Brunt [2] concerning the magnitude of the coefficient, K_R , of radiative diffusivity. Brunt originally computed K_R to be about $650 \text{ cm}^2 \text{ sec}^{-1}$ but in 1940, using the new absorption coefficients of Dennison, Ginsberg and Weber [4] he concluded that this value of K_R probably should be increased thirty-fold. The water vapor radiative transfer problem of this thesis used the Elsasser Atmospheric Radiation Chart which, in turn, is based primarily on the new absorption coefficients mentioned above. Actually K_R was not computed in this study but the results of this study form a basis which would permit the calculation fairly simply.

It was found also that carbon dioxide plays a surprisingly large part in the radiative heat transfer processes near the ground where rather large lapse rates are found. In the preparation of his radiation chart, Elsasser made the assumption that the carbon dioxide contribution to the net flux could be neglected in comparison to that due to water vapor. It turned out in this study that the radiative contribution to the rate of change of temperature due to carbon dioxide was in the neighborhood $1/3$ to $1/4$ that due to water vapor. Elsasser's remark, concerning the effect of carbon dioxide, "that even thin layers radiate as black bodies within these bands" was shown to be definitely invalid. In fact, using a formula for carbon

dioxide absorptivity due to Callendar [3], the computed absorptivities ranged anywhere from 2% to 20% for layers near the earth's surface, depending upon their thickness.

Surprisingly large values of turbulent temperature-change per half hour were obtained, in this study, at three inches above the ground. For example, there was a turbulent rate of cooling of 10°C per half-hour at 1300 local time. It was found, however, that even such large values were negligible insofar as affecting the magnitude of the coefficient of eddy conductivity in the surface layer. In other words, whenever the lapse rates were significantly different from dry adiabatic, it was found that the turbulent temperature-change term of the partial differential equation of eddy conduction was negligible in comparison to the turbulent heat flux through either boundary of a slab of air. Thus the surface layer extended at least to 80 feet throughout the period of this investigation and during the night extended to about 200 feet.

Other results deduced in this study are the following: The coefficient of eddy conductivity in the surface layer appears to follow a power law of the form $K = K_1 Z^m$, with $m \geq 1$ the exact value of m depending in some way upon the stability. Moreover in this layer, K takes on its maximum value at about 1300 LCT and its minimum value at about 1900 LCT.

II. THE NATURE OF THE DATA

1. The Data.

Data utilized in this research was taken from Report No. 29 compiled by the Electrical Engineering Research Laboratory of the University of Texas [6]. This report contains recorded measurements of temperature and vapor pressure for selected levels from the ground up to and including 288 feet. The soundings are recorded at half-hourly intervals throughout the 24 hour period chosen to represent a particular synoptic situation. Measurements of wind speed and direction are recorded for selected levels up to 307 feet. The sounding site is on level ground under cultivation.

The authors of [6] give the following statements of accuracy of the data.

(a) The temperatures are accurate to within 1°C over the $0-50^{\circ}\text{C}$ range.

(b) The 6-minute averaging period used to obtain temperatures is not sufficient to remove all turbulent fluctuations; however, they do not deviate more than $\pm 0.2^{\circ}\text{C}$ from the 30-minute mean temperature. This turbulent fluctuation of the 6-minute mean as compared with the 30-minute mean will be called "the gust error".

(c) The Aerovanes show a uniform response with an accuracy of $\pm 2\%$.

For a detailed description of the data and the field installation, the reader is referred to the report of the data [6].

2. Selection of Data for this Study.

The data for the period September 27-28, 1948 was selected for this study. A high pressure cell dominated the area and gave conditions of horizontal homogeneity.

Soundings at three-hourly intervals were used and computations of heat flux were made for the layers of air bounded by the ground, 6 and 18 inches; 3, 6, 12, 20, 35, 55, 80, 110, 145, 185, 235 and 288 feet, inasmuch as these are selected levels for which the temperature data were available.

1911-12 Sept 5-14

1912-13 Sept 15-24

1913-14 Oct 1-10

III. THEORETICAL AND EMPIRICAL CONCEPTS

1. The Water Vapor Radiative Transfer Problem.

Elsasser [5] gives a method for determining the net flux due to the water vapor content of a layer of atmosphere through the use of his radiation chart. The corrected optical depth of water vapor, u , in a column of air of unit cross-section is computed by using the formula:

$$u = - \frac{1}{1000} \sum q_i \sqrt{\frac{p_i}{1000}} \Delta_i p. \quad (3.1)$$

When only temperature and moisture data are available at given levels, pressures for these levels may be computed from the surface pressure by use of the integrated form of the hydrostatic equation:

$$g \Delta z = R_d \bar{T} (\ln p_1 - \ln p_2). \quad (3.2)$$

For the evaluation of net flux into or out of a slab of air, utilizing areas on Elsasser's Atmospheric Radiation Chart, Elsasser recommends the measurement of these areas by means of a planimeter. The difference of the net fluxes for a slab is then given in gram-calories per three hours by this method and is converted to rate of change of temperature of the slab by means of the equation:

$$F_2 - F_1 = -c_p(\Delta T) \frac{p_1 - p_2}{g}. \quad (3.3)$$

QUESTION 1

1. A system is shown in the figure below.

The system is a closed system and the boundary is fixed.

The system is a closed system and the boundary is fixed.

The system is a closed system and the boundary is fixed.

The system is a closed system and the boundary is fixed.

$$(1.1) \quad \frac{d}{dt} \int_{CV} \rho \frac{d}{dt} \left(\frac{1}{2} \mathbf{V} \cdot \mathbf{V} \right) dV = \sum \mathbf{F} \cdot \mathbf{V}$$

2. A system is shown in the figure below.

The system is a closed system and the boundary is fixed.

The system is a closed system and the boundary is fixed.

$$(2.1) \quad \frac{d}{dt} \int_{CV} \rho \frac{d}{dt} \left(\frac{1}{2} \mathbf{V} \cdot \mathbf{V} \right) dV = \sum \mathbf{F} \cdot \mathbf{V}$$

3. A system is shown in the figure below.

The system is a closed system and the boundary is fixed.

The system is a closed system and the boundary is fixed.

The system is a closed system and the boundary is fixed.

The system is a closed system and the boundary is fixed.

The system is a closed system and the boundary is fixed.

$$(3.1) \quad \frac{d}{dt} \int_{CV} \rho \frac{d}{dt} \left(\frac{1}{2} \mathbf{V} \cdot \mathbf{V} \right) dV = \sum \mathbf{F} \cdot \mathbf{V}$$

In this equation, F_2 is the net upward flux at the top of the slab, while F_1 is the net upward flux at the bottom of the slab. For further details concerning this method, reference should be made to Elsasser's study, Heat Transfer by Infrared Radiation in the Atmosphere [5].

2. The Carbon Dioxide Radiative Transfer Problem.

Callendar [3] gives formulas for the absorptivity in terms of the quantity of carbon dioxide for various wave bands of a parallel beam of radiation. His formulas for the equivalent thickness, c , of carbon dioxide, and for the monochromatic absorptivity of carbon dioxide, in a column of air of thickness Z , pressure P_a (in atmospheres) and temperature T (degrees absolute) are:

$$c = 8.7 Z p_a / T, \quad (3.4)$$

$$A = 1 - 1 / [1 + n (c \sqrt{p_a})^x]. \quad (3.5)$$

In equations (3.4) and (3.5), c is the length of absorbing path in cms of carbon dioxide at N.T.P. and is based on air having a normal carbon dioxide content (the partial pressure of carbon dioxide in the air now being .0032 atmospheres). The constants n and x are given for different limits of the intense absorption band centered at 15 microns.

Elsasser [5] states that, in the case of square-root absorption, a slab of thickness u is mathematically equivalent for diffuse radiation to

a linear column of length 1.78 u for beamed radiation. The condition of square-root absorption is satisfied for slabs of air of thickness 4 to 100 meters according to Panofsky [10]. For thinner layers, the factor 1.78 should be increased slightly; but the error introduced for such layers will not be great if the factor 1.78 is used. Inasmuch as diffuse radiation occurs in the atmosphere, slab thicknesses must be increased by the factor 1.78; which amounts to an increase in the equivalent thickness, c , of equation (3.4) by the factor 1.78. Utilizing this corrected equivalent thickness in the absorption formula (3.5) allows this formula to be applied to slab thicknesses of the atmosphere.

In this study, the rate of change of temperature of layers of air near the ground due to carbon dioxide as well as water vapor is to be determined. Furthermore, since the Atmospheric Radiation Chart of Elsasser is to be used for the rate of temperature-change resulting from water vapor, consideration must be given to his treatment of carbon dioxide. Elsasser [5] considers that the absorption by carbon dioxide occurs, for the most part, in the range 752 cm^{-1} to 584 cm^{-1} , that is, between 13.3 and 17.1 microns. He further considers that "very thin layers radiate as black bodies" and, therefore, neglects the radiative effects of carbon dioxide in comparison to those of water vapor, for problems concerning net flux. The chart, however, does give a separate representation of the black body flux contained within the strong band interval 13.3 - 17.1 microns. Callendar [3] gives the values $n = .35$ and $x = .55$ as suitable for determining the absorptivity by (5) within a band of limits 13.0 - 17.0 microns. It is assumed that the values of monochromatic absorptivity, A , determined from (3.4) and (3.5) are appropriate for the carbon dioxide limits of Elsasser, 13.3 - 17.1 microns.

Knowing the ground temperature and the mean temperature of the layers of atmosphere under consideration, the flux through the top boundary of each layer can be computed. For example, for the first slab above the ground, the equation of radiative transfer, sometimes called Schwarzschild's equation, gives

$$E = (1-A_1) E_{\lambda_0} + A_1 E_{\lambda_1} \quad , \quad (3.6)$$

where E is the flux through the top boundary of the layer, A_1 the monochromatic absorptivity of the layer, E_{λ_0} the black body flux in the band 13.3 - 17.1 microns at the temperature, T , of the ground (or the flux into the lower boundary) and E_{λ_1} is the black body flux at the mean temperature \bar{T} of the layer. Strictly speaking Schwarzschild's equation (3.6) is true for monochromatic intensity, or beamed flux, of radiation. Actually Elsasser [5] integrates the Schwarzschild equation in order to obtain the flux emerging from an arbitrary slab. He finds that this integration involves the computation of integrals $E_{i_3}(x) = \int_0^\infty \eta^{-3} e^{-\eta^x} d\eta$ where $\eta = \sec \psi$, values of which are given in [5]. However, he also shows that these computations imply the increase of the absorbing path by the factor 1.78 discussed above. It is therefore assumed that Schwarzschild's equation holds for fluxes E , E_{λ_0} , and E_{λ_1} with the value of absorptivity A corresponding to the absorbing path c replaced by 1.78 c , a result which Elsasser justifies.

For slabs above the first, equation (3.6) also permits the computation of upward flux E through the top boundary. However, for such computations E_{λ_0} must be taken to represent the flux into the bottom of the slab, which was that out of the top of the slab immediately below, E_{λ_1} would still represent the black body flux, in the band 13.3 - 17.1 microns, corresponding to the mean temperature of the slab under consideration.

...the ... of the ...

...the ... of the ...

$$(1.1) \quad \dots = \dots$$

...the ... of the ...

...the ... of the ...

...the ... of the ...

...the ... of the ...

...the ... of the ...

...the ... of the ...

...the ... of the ...

...the ... of the ...

In order to apply the same procedure to the problem of computing fluxes for the downward radiation of carbon dioxide as for the upward radiation, it is necessary to know the flux entering the top boundary of the highest layer. The top boundary is 288 feet for this study. Throughout the period used in this study, whenever a ground inversion exists, this height is very near the top of the inversion. The slope of the sounding above the ground inversion during this period is quite similar to that of the standard atmosphere. This remark is, on the whole, true also of the slope of the sounding above the 288 feet level during the hours in which no ground inversion is present. Therefore, the atmosphere from 10 kilometers is divided into slabs of approximately 100 meters thickness and having the appropriate temperature according to the standard atmospheric lapse rate. In treating equation (3.6), slab 1 is to be considered the topmost slab, slab 2 that immediately below, etc. It will be shown below that the amount of flux from above 10 kilometers produces negligible effect at the 288 foot level. Let flux E_0 enter the top of slab 1. The fluxes leaving the bottoms of the next several slabs are given by the following table.

<u>Slab</u>	<u>Flux through the lower boundary</u>	
1	$1 E_0 + a,$	
2	$m1 E_0 + ma + b,$	(3.7)
3	$nml E_0 + nma + nb + c.$	

In (3.7), 1, m, n..... etc. correspond to the factors. $(1-A_1)$, $(1-A_2)$, $(1-A_3)$, etc., respectively, of equation (3.6); a, b, c correspond to the values $A_1 E_{\lambda 1}$, $A_2 E_{\lambda 2}$, $A_3 E_{\lambda 3}$, etc. of equation (3.6).

... ..

... ..

... ..

... ..

... ..

... ..

... ..

... ..

... ..

... ..

... ..

... ..

... ..

... ..

... ..

... ..

... ..

... ..

... ..

... ..

... ..

... ..

... ..

... ..

... ..

... ..

Since, using equations (3.4) and (3.5), the average value of l , m , n , etc. is of the order 0.5 for a layer of thickness 100 meters, and E_0 is of the order of $10 \text{ cal cm}^{-2} (3 \text{ hr.})^{-1}$, it turns out that the contribution of the initial flux E_0 is negligible in treating equation (3.6) for the downward directed flux. We may therefore arbitrarily set $E_0 = 0$ in determining the flux through the bottom of the slabs and still obtain the correct result at 288 feet.

Finally, since we now may determine the amounts of upward and downward directed flux at every level, one can compute net-upward, net-downward and consequently net-outward directed flux, $F_2 - F_1$, for every consecutive pair of levels. This determines the radiative heating, or cooling, of the slab due to carbon dioxide radiation, and the actual rate of temperature-change can be computed, as before, from equation (3.3).

3. Heat Transfer by Molecular Conductivity.

The upward flux of heat due to molecular conduction is given by the formula:

$$F_m = -\alpha \frac{\partial T}{\partial Z} , \quad (3.8)$$

where α is the coefficient of molecular conductivity of air, and has the value $\alpha = 549(10)^{-7} \text{ cal cm}^{-1} \text{ sec}^{-1} \text{ T}^{-1}$ at 0°C , but is a function of temperature (c.f. for example, p. 44 of [1]).

It is necessary now only to compute upward fluxes F_{m2} and F_{m1} for the various slabs for which lapse rates are known, and again use equation (3.3) to convert net flux out of a slab into a corresponding rate of change of

temperature. In actual practice it is normally found, since α is very small, that in order to register a measurable net flux, the changes in lapse rates along the vertical must be quite extreme, and this can be expected only within the lowest two or three slabs.

4. Rate of Change of Temperature by Eddy Conductivity.

The formula for the observed rate of temperature change is:

$$\frac{\partial T}{\partial t} = \left(\frac{\partial T}{\partial t}\right)_w + \left(\frac{\partial T}{\partial t}\right)_c + \left(\frac{\partial T}{\partial t}\right)_m + \left(\frac{\partial T}{\partial t}\right)_t, \quad (3.9)$$

where $\left(\frac{\partial T}{\partial t}\right)_w$ is due to water vapor,

$\left(\frac{\partial T}{\partial t}\right)_c$ is due to carbon dioxide,

$\left(\frac{\partial T}{\partial t}\right)_m$ is due to molecular conduction,

$\left(\frac{\partial T}{\partial t}\right)_t$ is due to eddy conduction.

The observed rate of change of temperature per half-hour is given for each layer by the data used in this study. As a result of methods previously described, the only unknown of formula (3.8) is the rate of change of temperature due to eddy conduction.

5. The Coefficient of Eddy Conduction.

The net-outward flux for a layer of atmosphere due to turbulent conduction may be expressed as:

$$K_1 \rho_1 c_p \left(\frac{\partial \theta}{\partial z}\right)_1 - K_2 \rho_2 c_p \left(\frac{\partial \theta}{\partial z}\right)_2 = c_p \left(\frac{\partial T}{\partial t}\right)_t \frac{\rho_1 - \rho_2}{g}. \quad (3.10)$$

In (3.10) K_2 and K_1 are the coefficients of eddy conductivity at the top and bottom of any slab of atmosphere, respectively. Making the substitutions

$$\rho = \frac{p}{RT} \div \frac{p_m}{RT}$$

and

$$\frac{\partial \theta}{\partial Z} = \frac{\theta}{T} \left(\frac{\partial T}{\partial Z} + \gamma_d \right) \div \left(\frac{\partial T}{\partial Z} + \gamma_d \right) ,$$

both approximations being valid to within 1% for the layers between the surface and 288 feet, we obtain:

$$2.93 \left(\frac{\partial T}{\partial x} \right)_x \frac{p_1 - p_2}{g} = \frac{K_1}{T_1} \left(\frac{\partial T}{\partial Z} + \gamma_d \right)_1 - \frac{K_2}{T_2} \left(\frac{\partial T}{\partial Z} + \gamma_d \right)_2. \quad (3.11)$$

In (3.11), all items labeled with subscript 1 refer to measurements made at the center of slab 1, all items with subscript 2 refer to the center of slab 2; p_m is the mean of p_1 and p_2 . Thus (3.11) determines the rate of change of temperature approximately at the boundary of slab 1 and slab 2. In general, slab 1 will denote any lower slab and slab 2 the slab immediately above slab 1. Thus (3.11) may be used as a recursion formula to determine all values of K_i after K_{i-1} has been determined. The only limitation on its use arises when $-\frac{\partial T}{\partial Z} = \gamma_d$, that is, when the lapse rate of the slab is dry adiabatic, or, not significantly different from γ_d .

In using (3.11) as a recursion formula, it is necessary to determine a value of K at some specific level to permit determination of all other K_i . In order to do this without making too many assumptions, a value of K at

some standard level can be determined by reference to the theory of momentum-transfer within the surface layer. The coefficient of eddy viscosity can be determined at a standard level, say 16 feet, and it can be assumed to give a representative value of the coefficient of eddy conductivity. The particular values of K will then depend to some extent on momentum-transfer theory, but the comparative values reflect only the measurements of eddy conductivity. Recent results of Lottau [9] are drawn upon for the purpose of finding a value of K at some standard level.

According to the Prandtl theory of momentum-transfer*, one obtains:

$$K = \ell^2 \left(\frac{\partial \bar{u}}{\partial Z} \right). \quad (3.12)$$

In (3.12) ℓ is the mean mixing length and $\frac{\partial \bar{u}}{\partial Z}$ is the observed shear of the horizontal wind, both measured at a given level. Lettau [9] gives the following formulas which permit the calculation of the coefficient of eddy viscosity within the surface layer:

$$\ell = \ell_a / \left[1 + \frac{\partial \theta}{\partial Z} / \theta'_c \right], \quad \ell_a = k (Z + Z_0), \quad (3.13)$$

where

$$\theta'_c = \frac{T_m}{g} \left(\frac{\partial \bar{u}_a}{\partial Z} \right)^2. \quad (3.14)$$

*Haurwitz, B. Dynamic Meteorology. Equation (74.2). McGraw-Hill 1941.

The first part of the paper is devoted to the study of the
 properties of the function $f(x)$ defined by the equation

$$f(x) = \int_0^x \frac{1}{1+t^2} dt$$
 and to the proof of the following theorem:
 The function $f(x)$ is continuous and differentiable
 on the interval $(-\infty, \infty)$ and its derivative is

$$f'(x) = \frac{1}{1+x^2}$$
 The second part of the paper is devoted to the study of the
 properties of the function $g(x)$ defined by the equation

$$g(x) = \int_0^x \frac{1}{1+t^4} dt$$
 and to the proof of the following theorem:
 The function $g(x)$ is continuous and differentiable
 on the interval $(-\infty, \infty)$ and its derivative is

$$g'(x) = \frac{1}{1+x^4}$$

The third part of the paper is devoted to the study of the
 properties of the function $h(x)$ defined by the equation

$$h(x) = \int_0^x \frac{1}{1+t^6} dt$$
 and to the proof of the following theorem:
 The function $h(x)$ is continuous and differentiable
 on the interval $(-\infty, \infty)$ and its derivative is

$$h'(x) = \frac{1}{1+x^6}$$
 The fourth part of the paper is devoted to the study of the
 properties of the function $k(x)$ defined by the equation

$$k(x) = \int_0^x \frac{1}{1+t^8} dt$$
 and to the proof of the following theorem:
 The function $k(x)$ is continuous and differentiable
 on the interval $(-\infty, \infty)$ and its derivative is

$$k'(x) = \frac{1}{1+x^8}$$

The fifth part of the paper is devoted to the study of the
 properties of the function $l(x)$ defined by the equation

$$l(x) = \int_0^x \frac{1}{1+t^{10}} dt$$
 and to the proof of the following theorem:
 The function $l(x)$ is continuous and differentiable
 on the interval $(-\infty, \infty)$ and its derivative is

$$l'(x) = \frac{1}{1+x^{10}}$$
 The sixth part of the paper is devoted to the study of the
 properties of the function $m(x)$ defined by the equation

$$m(x) = \int_0^x \frac{1}{1+t^{12}} dt$$
 and to the proof of the following theorem:
 The function $m(x)$ is continuous and differentiable
 on the interval $(-\infty, \infty)$ and its derivative is

$$m'(x) = \frac{1}{1+x^{12}}$$

The seventh part of the paper is devoted to the study of the
 properties of the function $n(x)$ defined by the equation

$$n(x) = \int_0^x \frac{1}{1+t^{14}} dt$$
 and to the proof of the following theorem:
 The function $n(x)$ is continuous and differentiable
 on the interval $(-\infty, \infty)$ and its derivative is

$$n'(x) = \frac{1}{1+x^{14}}$$
 The eighth part of the paper is devoted to the study of the
 properties of the function $o(x)$ defined by the equation

$$o(x) = \int_0^x \frac{1}{1+t^{16}} dt$$
 and to the proof of the following theorem:
 The function $o(x)$ is continuous and differentiable
 on the interval $(-\infty, \infty)$ and its derivative is

$$o'(x) = \frac{1}{1+x^{16}}$$

In (3.13) and (3.14), the subscript "a" indicates an isotropic or adiabatic surface layer. T_m is the mean temperature of the slab for which $\frac{\partial \theta}{\partial Z}$ has been determined. The value of $\frac{\partial u_a}{\partial Z}$ may be determined by the well-known logarithmic law

$$u_a = \frac{1}{k} \sqrt{\frac{\tau_a}{\rho}} \ln \left(\frac{Z + Z_0}{Z_0} \right) , \quad (3.15)$$

$$\frac{\partial u_a}{\partial Z} = \sqrt{\frac{\tau_a}{\rho}} \frac{1}{k(Z + Z_0)} . \quad (3.16)$$

In (3.15) and (3.16), all variables are understood to refer to the surface layer. For example,

τ_a is the constant value of the stress,

u_a is the horizontal wind speed,

l_a is the mixing length,

k is the Von Karman constant, $k = .45$,

Z_0 is the roughness parameter.

The values of Z_0 and $\sqrt{\frac{\tau_a}{\rho}}$ can be obtained from a plot of $\frac{\partial u_a}{\partial Z}$ when adiabatic conditions are found. Observations of Lettau [8] indicate that such conditions exist at sunrise and sunset. An average u_a profile, therefore, can be drawn based on both sunrise and sunset data in order to determine Z_0 and the mean value of $\sqrt{\frac{\tau_a}{\rho}}$ for the day.

IV. RATES OF CHANGE OF TEMPERATURE

1. Rate of Change of Temperature Due to Water Vapor.

Radiation transfer due to water vapor was computed for each layer of the soundings chosen from the data by the method described in Chapter III, Section 1, of this study. This method requires a knowledge of the specific humidity at each level. The data [6] gives the vapor pressure at each level. These vapor pressures were converted to specific humidity by use of the Kiefer Multi-Pressure Hygrometric Chart. Since equation (3.1) requires the pressure-thickness, Δp , of all layers it was necessary to compute the pressure at every level by equation (3.2). To do this, the surface pressure must be known. The surface pressure was computed from the sea level pressure recorded for Austin, Texas on the surface map at the middle of the period under study, 27-28 September 1948. This was done by reversing the procedure of the reduction of pressures to sea level, knowing the height of the base of the tower (525 feet MSL).

A (u,T) relationship was computed for all levels of the soundings and plotted on the Elsasser Chart. The difference of the net fluxes of each slab of the soundings was obtained by making the required area measurements with the aid of a planimeter. Figures 1 and 2 show schematically the areas that represent the differences of net flux, for one slab of atmosphere for the following cases:

(a) The slab lies within a ground inversion (Figure 1).

(b) The temperature decreases with height (Figure 2).

In Figures 1 and 2, the reference levels L_1 and L_2 denote respectively the bottom and top of the slab, both taken to lie below the 288 foot level.

ATMOSPHERIC RADIATION CHART

SECOND REVISED EDITION

DEVELOPED IN COOPERATION WITH THE

U.S. WEATHER BUREAU AT THE

CALIFORNIA INSTITUTE OF

TECHNOLOGY AND THE BLUE

HILL OBSERVATORY OF

HARVARD UNIVERSITY

WATER	+40°	+30°	+20°	+10°	0°	-10°	-20°	-30°	-40°	-50°	-60°	-70°	-80°	WATER
BLACK	141.4	124.2	108.6	94.5	81.9	70.5	60.4	51.4	43.5	36.5	30.4	25.0	20.5	BLACK
CO ₂	117.4	102.6	89.3	77.4	66.8	57.4	49.1	41.8	35.4	29.8	24.9	20.7	17.1	CO ₂
0.00025	111.0	96.7	83.8	72.4	62.2	53.1	45.1	38.1	32.0	26.7	22.1	18.1	14.8	0.00025
0.0006	106.8	92.9	80.4	69.2	59.3	50.5	42.7	36.0	30.0	24.9	20.5	16.7	13.5	0.0006
0.001	103.5	89.9	77.7	66.9	57.2	48.6	41.1	34.5	28.7	23.7	19.4	15.6	12.7	0.001
0.0025	96.6	83.7	72.2	61.9	52.8	44.7	37.6	31.4	26.0	21.3	17.3	13.9	11.1	0.0025
0.004	92.4	80.0	68.9	59.1	50.3	42.5	35.7	29.7	24.5	20.0	16.2	13.0	10.2	0.004
0.006	88.6	76.7	66.0	56.4	48.0	40.5	33.9	28.1	23.1	18.8	15.2	12.1	9.5	0.006
0.01	83.4	72.1	62.0	53.0	44.9	37.8	31.6	26.1	21.4	17.3	13.9	11.0	8.6	0.01
0.015	79.5	68.7	59.0	50.3	42.6	35.8	29.9	24.6	20.1	16.2	12.9	10.2	7.9	0.015
0.025	74.2	64.1	54.9	46.8	39.6	33.2	27.5	22.6	18.4	14.8	11.7	9.1	7.0	0.025
0.04	69.4	59.8	51.3	43.6	36.8	30.8	25.5	20.9	17.0	13.6	10.7	8.3	6.3	0.04
0.06	65.2	56.2	48.1	40.8	34.4	28.7	23.7	19.4	15.6	12.4	9.7	7.5	5.7	0.06
0.1	59.7	51.4	43.9	37.2	31.3	26.0	21.4	17.4	14.0	11.1	8.6	6.6	4.9	0.1
0.15	55.1	47.4	40.5	34.3	28.7	23.9	19.6	15.9	12.7	10.0	7.8	5.9	4.4	0.15
0.25	49.2	42.2	36.0	30.4	25.5	21.1	17.3	14.0	11.2	8.8	6.7	5.1	3.7	0.25
0.4	43.9	37.6	32.0	27.0	22.5	18.6	15.2	12.3	9.8	7.6	5.8	4.4	3.2	0.4
0.6	39.5	33.8	28.7	24.1	20.1	16.6	13.5	10.9	8.6	6.7	5.1	3.8	2.8	0.6
1.0	34.0	29.1	24.7	20.8	17.3	14.3	11.6	9.4	7.4	5.7	4.4	3.2	2.3	1.0
1.5	30.0	25.7	21.8	18.3	15.2	12.5	10.2	8.2	6.5	5.0	3.8	2.8	2.0	1.5
2.5	25.0	21.3	18.1	15.2	12.6	10.4	8.4	6.8	5.3	4.1	3.1	2.3	1.6	2.5
4	20.5	17.5	14.8	12.4	10.3	8.5	6.9	5.5	4.4	3.4	2.5	1.9	1.3	4
6	16.5	14.0	11.9	9.9	8.3	6.8	5.5	4.4	3.5	2.7	2.1	1.5	1.1	6
10	11.4	9.6	8.1	6.7	5.6	4.6	3.8	3.0	2.4	1.9	1.4	1.0	0.7	10
15	7.9	6.6	5.5	4.5	3.7	3.1	2.5	2.0	1.6	1.2	0.9	0.7	0.5	15
25	4.6	3.8	3.1	2.5	2.0	1.6	1.3	1.0	0.8	0.7	0.5	0.4	0.3	25
WATER	+40°	+30°	+20°	+10°	0°	-10°	-20°	-30°	-40°	-50°	-60°	-70°	-80°	WATER

UNIT LENGTH

UNIT AREA: FLUX OF 1 CAL/CM²/3 HOURS

COOLING $\Delta T = 4.1(f_1 - f_2)/(p_1 - p_2)$

TYPICAL NIGHTTIME CONDITIONS

positive area (cooling)

negative area (warming)

Difference of Net Fluxes for a Slab Below 288 Feet

Figure 1



ATMOSPHERIC RADIATION CHART

SECOND REVISED EDITION

DEVELOPED IN COOPERATION WITH THE

U.S. WEATHER BUREAU AT THE

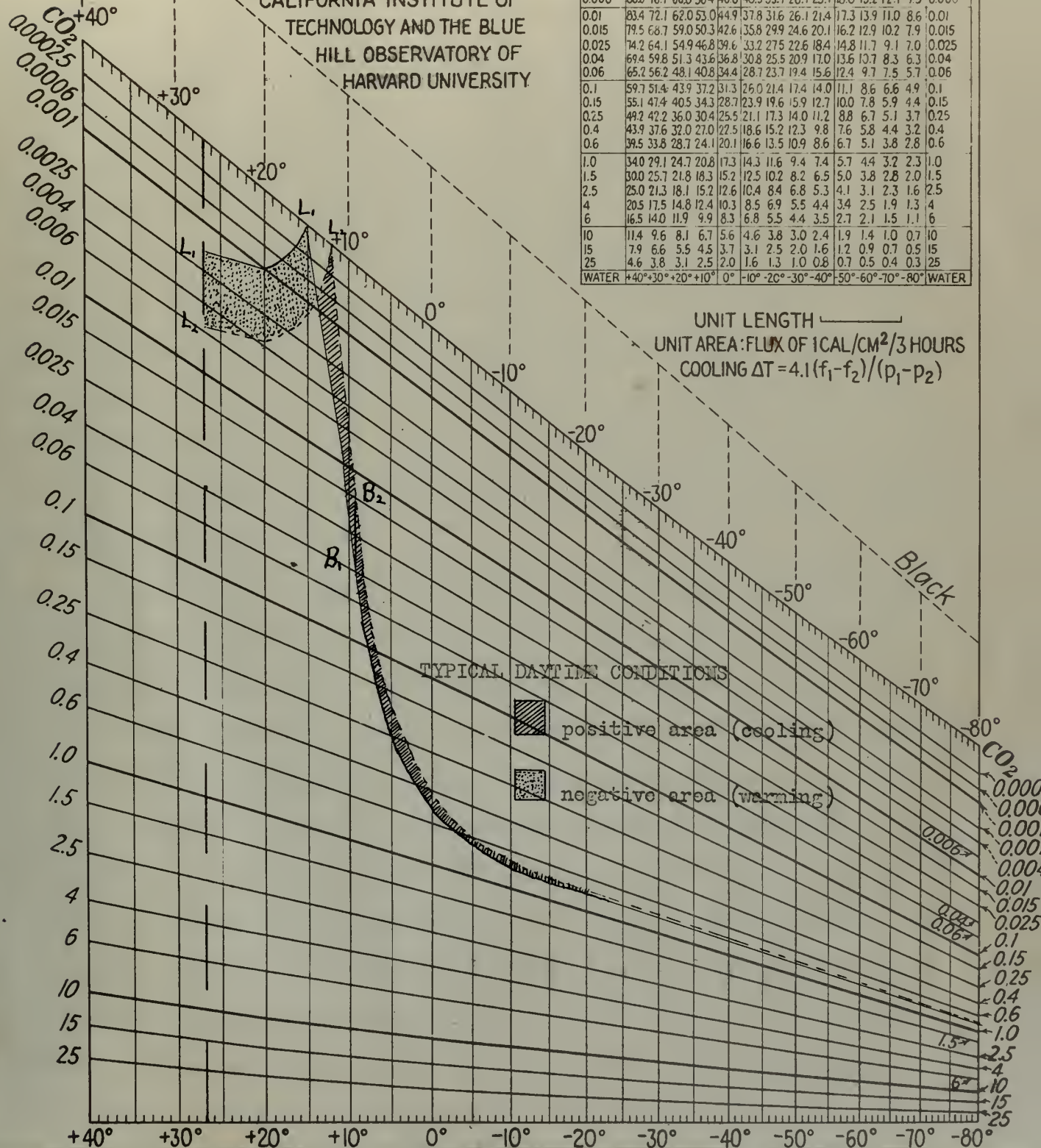
CALIFORNIA INSTITUTE OF

TECHNOLOGY AND THE BLUE

HILL OBSERVATORY OF

HARVARD UNIVERSITY

WATER	+40°	+30°	+20°	+10°	0°	-10°	-20°	-30°	-40°	-50°	-60°	-70°	-80°	WATER
BLACK	1414	1242	1085	945	819	705	604	514	435	365	304	250	205	167
CO ₂	1174	1026	893	774	668	574	491	418	354	298	249	207	171	140
0.00025	1110	967	838	724	622	531	451	381	320	267	221	181	148	0.00025
0.0006	1068	929	804	692	593	505	427	360	300	249	205	167	135	0.0006
0.001	1035	899	777	669	572	486	411	345	287	237	194	158	127	0.001
0.0025	966	837	722	619	528	447	376	314	260	213	173	139	111	0.0025
0.004	924	800	689	591	503	425	357	297	245	200	162	130	102	0.004
0.006	886	767	660	564	480	405	339	281	231	188	152	121	95	0.006
0.01	834	721	620	530	449	378	316	261	214	173	139	110	86	0.01
0.015	795	687	590	503	426	358	299	246	201	162	129	102	79	0.015
0.025	742	641	549	468	396	332	275	226	184	148	117	91	70	0.025
0.04	694	598	513	436	368	308	255	209	170	136	107	83	63	0.04
0.06	652	562	481	408	344	287	237	194	156	124	97	75	57	0.06
0.1	597	514	439	372	313	260	214	174	140	111	86	66	49	0.1
0.15	551	474	405	343	287	239	196	159	127	100	78	59	44	0.15
0.25	492	422	360	304	255	211	173	140	112	88	67	51	37	0.25
0.4	439	376	320	270	225	186	152	123	98	76	58	44	32	0.4
0.6	395	338	287	241	201	166	135	109	86	67	51	38	28	0.6
1.0	340	291	247	208	173	143	116	94	74	57	44	32	23	1.0
1.5	300	257	218	183	152	125	102	82	65	50	38	28	20	1.5
2.5	250	213	181	152	126	104	84	68	53	41	31	23	16	2.5
4	205	175	148	124	103	85	69	55	44	34	25	19	13	4
6	165	140	119	99	83	68	55	44	35	27	21	15	11	6
10	114	96	81	67	56	46	38	30	24	19	14	10	07	10
15	79	66	55	45	37	31	25	20	16	12	09	07	05	15
25	46	38	31	25	20	16	13	10	08	07	05	04	03	25
WATER	+40°	+30°	+20°	+10°	0°	-10°	-20°	-30°	-40°	-50°	-60°	-70°	-80°	WATER



Difference of Net Fluxes for a Slab Below 268 Feet

Figure 2.

Consider next Figure 1. The (u,T) curve extending above L_1 must eventually cross that above L_2 because the former curve eventually corresponds to a greater integrated optical depth of water vapor. Suppose this "cross-over" point is labeled A. At 2200 LCT, the complete radiosonde was available to supplement the 2200 micrometeorological sounding. It was found that the cross-over points for the (u,T) plots above the slab levels L_1 and L_2 occurred from about 300 feet for the lower, thinner slabs to about 800 feet for the higher, thicker slabs. Moreover, it was found that the area computation made by terminating the (u,T) curves above L_1 and L_2 at points B_1 and B_2 corresponding to the 288 feet level was in error only by 2-7% when compared with the areas given by the complete (u,T) curves. This small error is due to a tendency of positive and negative areas below the isotherm B_1B_2 to cancel each other.

Consider next Figure 2, representing typical daytime conditions. No exact comparison is known here of the error made in neglecting the area below and to the right of the isotherm B_1B_2 . No cross-over point occurs in this case so there is no tendency for cancellation of positive and negative areas. For the lower, thinner slabs little error could occur because the (u,T) curves above the slab boundaries are in general nearly coincident at B_1 and B_2 . The greatest error should occur in the slab 185-235 feet and the error should be progressively smaller in the slabs immediately below. The neglected area, if appreciable, should cause a reduced amount of cooling or increased warming in the midday hours in the slab 185-235 feet. Actually Table 1 shows no evidence of reduced cooling of the slab 185-235 feet. For the ratio of the 1300 LCT cooling of this slab to those of the three slabs immediately below is almost identical with the corresponding slab ratios of the 2200 LCT sounding, whose values are known to be correct.

...the

...the

...the

...the

...the

...the

...the

...the

...the

...the

...the

...the

...the

...the

...the

...the

...the

...the

...the

...the

...the

...the

...the

...the

...the

...the

...the

...the

(Times given in LCT.)

Layer (in feet)	0200 ΔF	0500 ΔF	0800 ΔF	1100 ΔF	1300 ΔF	1600 ΔF	1900 ΔF	2200 ΔF
0-.5	.01	-.01	.03	.04	.02	.00	-.045	.00
.5-1.5	.045	.05	-.04	-.40	-.38	-.175	-.02	.04
1.5-3.0	.065	.065	-.10	-.44	-.48	-.21	.03	.04
3-6	.08	.08	-.22	-.56	-.51	-.28	.05	.10
6-12	.10	.10	-.23	-.87	-.67	-.38	.11	.08
12-20	.08	.11	-.17	-.66	-.75	-.38	.19	.08
20-35	.10	.10	-.21	-.80	-.79	-.34	.23	.08
35-55	.08	.10	-.24	-.82	-.79	-.35	.33	.11
55-80	.02	.08	-.29	-.66	-.56	-.32	.26	.19
80-110	.04	.07	-.02	-.61	-.60	-.34	.28	.32
110-145	.13	.09	-.07	-.54	-.59	-.31	.21	.36
145-185	.19	.25	-.33	-.56	-.57	-.28	.20	.29
185-235	.21	.26	-.17	-.45	-.46	-.28	.20	.28

Heat Transfer Due to Water Vapor, cal. (3 hr.)⁻¹

TABLE 1.

Table 1.1 (continued)

Order	Year	1970	1971	1972	1973	1974	1975	Total
1.	1970	100	100	100	100	100	100	600
2.	1971	100	100	100	100	100	100	600
3.	1972	100	100	100	100	100	100	600
4.	1973	100	100	100	100	100	100	600
5.	1974	100	100	100	100	100	100	600
6.	1975	100	100	100	100	100	100	600
7.	1976	100	100	100	100	100	100	600
8.	1977	100	100	100	100	100	100	600
9.	1978	100	100	100	100	100	100	600
10.	1979	100	100	100	100	100	100	600
11.	1980	100	100	100	100	100	100	600
12.	1981	100	100	100	100	100	100	600
13.	1982	100	100	100	100	100	100	600
14.	1983	100	100	100	100	100	100	600
15.	1984	100	100	100	100	100	100	600
16.	1985	100	100	100	100	100	100	600
17.	1986	100	100	100	100	100	100	600
18.	1987	100	100	100	100	100	100	600
19.	1988	100	100	100	100	100	100	600
20.	1989	100	100	100	100	100	100	600

Source: U.S. Department of Commerce, Bureau of Economic Analysis.

U.S. DEPARTMENT OF COMMERCE

(Times given in LCT.)

Layer (in feet)	0200 (°C)	0500 (°C)	0800 (°C)	1100 (°C)	1300 (°C)	1600 (°C)	1900 (°C)	2200 (°C)
0-.5	-2.28	2.28	-6.83	- 9.65	- 5.47	.00	10.25	.00
.5-1.5	-5.12	-5.54	4.56	46.86	39.83	20.50	2.28	-4.56
1.5-3.0	-4.94	-4.84	6.41	34.04	37.13	16.24	-2.28	-3.04
3.0-6	-3.01	-3.01	8.35	21.87	19.91	10.93	-1.92	-3.80
6-12	-1.88	-1.88	4.39	16.90	13.08	7.35	-2.11	-1.52
12-20	-1.13	-1.55	2.43	9.63	10.90	5.56	-2.74	-1.14
20-35	- .75	- .75	1.59	6.18	6.20	2.64	-1.76	- .61
35-55	- .44	- .56	1.37	4.77	4.59	2.04	-1.91	- .61
55-80	- .09	- .36	1.32	3.08	2.61	1.50	-1.21	- .88
80-110	- .15	- .26	.76	2.35	2.38	1.31	-1.08	-1.24
110-145	- .43	- .29	.23	1.80	1.97	1.04	- .70	-1.20
145-185	- .54	- .70	.93	1.73	1.63	.81	- .58	- .83
185-235	- .52	- .63	.41	1.05	1.14	.70	- .50	- .69

Three-hourly Rate of Change of Temperature Due to Water Vapor

TABLE 2.

Table 1 gives the values obtained for heat transfer due to water vapor in cal. (3 hr.)^{-1} . Table 2 gives the three-hourly rate of change of temperature for each layer of each sounding, computed from Table 1 by use of equation (3.3).

2. Rate of Change of Temperature Due to Carbon Dioxide.

The differences in upward-directed flux due to the radiative transfer of carbon dioxide, in the band 13.3 - 17.1 microns, were computed for each layer by the use of equation (3.6). The differences in downward-directed flux were obtained from the method of Chapter III, Section 2.

The computations of downward-directed flux took into account that the mid-period sounding was, on an average, ten degrees warmer throughout than that of the standard atmosphere, although the slope was assumed to be that of the standard atmosphere. This amounted to increasing the average emission from the layers by the factor 10%, which factor is the percentage increase in flux $E_{\lambda 1}$ of equation (3.6) due to the increase in the mean temperature, T_m , of each layer compared to the standard atmospheric temperature. The adjusted value obtained for the flux through the top boundary of the layer 288-235 feet was $18.79 \text{ cal cm}^{-2} \text{ (3 hr.)}^{-1}$. This value was used as a constant value, for the period of this study and computations of flux differences for the layers of each sounding under study were made using equation (3.6). The values of black body flux of emission for the carbon dioxide band 13.3 - 17.1 microns, at the mean temperature of each slab were taken from the top of the Atmospheric Radiation Chart. The values of monochromatic absorptivity were computed using equation (3.4) and (3.5).

1. The first part of the paper is devoted to the study of the properties of the function $f(x)$ defined by the equation $f(x) = \sum_{n=0}^{\infty} \frac{x^n}{n!}$. It is shown that $f(x)$ is a continuous function and that $f(x) = e^x$ for all x .

2. In the second part of the paper, we study the properties of the function $g(x)$ defined by the equation $g(x) = \sum_{n=0}^{\infty} \frac{x^n}{n!} \cos \frac{x^n}{n!}$. It is shown that $g(x)$ is a continuous function and that $g(x) = e^x \cos x$ for all x .

3. In the third part of the paper, we study the properties of the function $h(x)$ defined by the equation $h(x) = \sum_{n=0}^{\infty} \frac{x^n}{n!} \sin \frac{x^n}{n!}$. It is shown that $h(x)$ is a continuous function and that $h(x) = e^x \sin x$ for all x .

4. In the fourth part of the paper, we study the properties of the function $k(x)$ defined by the equation $k(x) = \sum_{n=0}^{\infty} \frac{x^n}{n!} \cos \frac{x^n}{n!} \sin \frac{x^n}{n!}$. It is shown that $k(x)$ is a continuous function and that $k(x) = e^x \cos x \sin x$ for all x .

5. In the fifth part of the paper, we study the properties of the function $l(x)$ defined by the equation $l(x) = \sum_{n=0}^{\infty} \frac{x^n}{n!} \sin \frac{x^n}{n!} \cos \frac{x^n}{n!}$. It is shown that $l(x)$ is a continuous function and that $l(x) = e^x \sin x \cos x$ for all x .

6. In the sixth part of the paper, we study the properties of the function $m(x)$ defined by the equation $m(x) = \sum_{n=0}^{\infty} \frac{x^n}{n!} \cos \frac{x^n}{n!} \sin \frac{x^n}{n!} \cos \frac{x^n}{n!}$. It is shown that $m(x)$ is a continuous function and that $m(x) = e^x \cos x \sin x \cos x$ for all x .

7. In the seventh part of the paper, we study the properties of the function $n(x)$ defined by the equation $n(x) = \sum_{n=0}^{\infty} \frac{x^n}{n!} \sin \frac{x^n}{n!} \cos \frac{x^n}{n!} \sin \frac{x^n}{n!}$. It is shown that $n(x)$ is a continuous function and that $n(x) = e^x \sin x \cos x \sin x$ for all x .

(Times given in LCT.)

Layer (in feet)	0200 ΔF	0500 ΔF	0800 ΔF	1100 ΔF	1300 ΔF	1600 ΔF	1900 ΔF	2200 ΔF
0-.5	-.012	-.010	-.00	-.010	-.010	-.003	-.025	-.010
.5-1.5	-.005	-.007	-.015	-.064	-.062	-.030	-.021	-.005
1.5-3.0	-.001	-.002	-.027	-.101	-.094	-.044	-.007	-.005
3.0-6.0	.004	.003	-.042	-.149	-.133	-.062	.010	.002
6-12	.015	.016	-.049	-.211	-.187	-.083	.048	.015
12-20	.012	.013	-.053	-.216	-.222	-.089	.074	.018
20-35	.012	.008	-.080	-.269	-.285	-.113	.113	.031
35-55	.022	.010	-.095	-.368	-.286	-.114	.155	.064
55-80	.023	.005	-.102	-.232	-.257	-.106	.169	.122
80-110	.044	.006	-.066	-.207	-.241	-.092	.174	.185
110-145	.092	.023	-.082	-.184	-.224	-.056	.184	.208
145-185	.127	.051	-.124	-.115	-.159	-.003	.210	.212
185-235	.165	.092	-.126	-.037	-.087	.061	.246	.231

Heat Transfer Due to Carbon Dioxide, Cal.(3 hr.)⁻¹

TABLE 3.

Table 1. Summary of data for the first 1000 cases.

Case No.	Age	Sex	Occupation	Marital Status	Religion	Ethnicity	Language	Country of Origin
1	25	M	Student	Single	Christian	White	English	USA
2	30	F	Teacher	Married	Muslim	Black	Arabic	USA
3	45	M	Engineer	Married	Jewish	White	Hebrew	USA
4	55	F	Homemaker	Married	Catholic	White	Spanish	USA
5	60	M	Retired	Married	Buddhist	Asian	Chinese	USA
6	65	F	Retired	Married	Hindu	Asian	Hindi	USA
7	70	M	Retired	Married	Sikh	Asian	Punjabi	USA
8	75	F	Retired	Married	Orthodox	White	Russian	USA
9	80	M	Retired	Married	Protestant	White	German	USA
10	85	F	Retired	Married	Catholic	White	Italian	USA
11	90	M	Retired	Married	Orthodox	White	Greek	USA
12	95	F	Retired	Married	Catholic	White	Irish	USA
13	100	M	Retired	Married	Protestant	White	Scottish	USA
14	105	F	Retired	Married	Catholic	White	Welsh	USA
15	110	M	Retired	Married	Orthodox	White	Polish	USA
16	115	F	Retired	Married	Catholic	White	Czech	USA
17	120	M	Retired	Married	Protestant	White	Slovak	USA
18	125	F	Retired	Married	Catholic	White	Hungarian	USA
19	130	M	Retired	Married	Orthodox	White	Romanian	USA
20	135	F	Retired	Married	Catholic	White	Bulgarian	USA
21	140	M	Retired	Married	Protestant	White	Serbian	USA
22	145	F	Retired	Married	Catholic	White	Croatian	USA
23	150	M	Retired	Married	Orthodox	White	Slovenian	USA
24	155	F	Retired	Married	Catholic	White	Czech	USA
25	160	M	Retired	Married	Protestant	White	Slovak	USA
26	165	F	Retired	Married	Catholic	White	Hungarian	USA
27	170	M	Retired	Married	Orthodox	White	Romanian	USA
28	175	F	Retired	Married	Catholic	White	Bulgarian	USA
29	180	M	Retired	Married	Protestant	White	Serbian	USA
30	185	F	Retired	Married	Catholic	White	Croatian	USA
31	190	M	Retired	Married	Orthodox	White	Slovenian	USA
32	195	F	Retired	Married	Catholic	White	Czech	USA
33	200	M	Retired	Married	Protestant	White	Slovak	USA
34	205	F	Retired	Married	Catholic	White	Hungarian	USA
35	210	M	Retired	Married	Orthodox	White	Romanian	USA
36	215	F	Retired	Married	Catholic	White	Bulgarian	USA
37	220	M	Retired	Married	Protestant	White	Serbian	USA
38	225	F	Retired	Married	Catholic	White	Croatian	USA
39	230	M	Retired	Married	Orthodox	White	Slovenian	USA
40	235	F	Retired	Married	Catholic	White	Czech	USA
41	240	M	Retired	Married	Protestant	White	Slovak	USA
42	245	F	Retired	Married	Catholic	White	Hungarian	USA
43	250	M	Retired	Married	Orthodox	White	Romanian	USA
44	255	F	Retired	Married	Catholic	White	Bulgarian	USA
45	260	M	Retired	Married	Protestant	White	Serbian	USA
46	265	F	Retired	Married	Catholic	White	Croatian	USA
47	270	M	Retired	Married	Orthodox	White	Slovenian	USA
48	275	F	Retired	Married	Catholic	White	Czech	USA
49	280	M	Retired	Married	Protestant	White	Slovak	USA
50	285	F	Retired	Married	Catholic	White	Hungarian	USA
51	290	M	Retired	Married	Orthodox	White	Romanian	USA
52	295	F	Retired	Married	Catholic	White	Bulgarian	USA
53	300	M	Retired	Married	Protestant	White	Serbian	USA
54	305	F	Retired	Married	Catholic	White	Croatian	USA
55	310	M	Retired	Married	Orthodox	White	Slovenian	USA
56	315	F	Retired	Married	Catholic	White	Czech	USA
57	320	M	Retired	Married	Protestant	White	Slovak	USA
58	325	F	Retired	Married	Catholic	White	Hungarian	USA
59	330	M	Retired	Married	Orthodox	White	Romanian	USA
60	335	F	Retired	Married	Catholic	White	Bulgarian	USA
61	340	M	Retired	Married	Protestant	White	Serbian	USA
62	345	F	Retired	Married	Catholic	White	Croatian	USA
63	350	M	Retired	Married	Orthodox	White	Slovenian	USA
64	355	F	Retired	Married	Catholic	White	Czech	USA
65	360	M	Retired	Married	Protestant	White	Slovak	USA
66	365	F	Retired	Married	Catholic	White	Hungarian	USA
67	370	M	Retired	Married	Orthodox	White	Romanian	USA
68	375	F	Retired	Married	Catholic	White	Bulgarian	USA
69	380	M	Retired	Married	Protestant	White	Serbian	USA
70	385	F	Retired	Married	Catholic	White	Croatian	USA
71	390	M	Retired	Married	Orthodox	White	Slovenian	USA
72	395	F	Retired	Married	Catholic	White	Czech	USA
73	400	M	Retired	Married	Protestant	White	Slovak	USA
74	405	F	Retired	Married	Catholic	White	Hungarian	USA
75	410	M	Retired	Married	Orthodox	White	Romanian	USA
76	415	F	Retired	Married	Catholic	White	Bulgarian	USA
77	420	M	Retired	Married	Protestant	White	Serbian	USA
78	425	F	Retired	Married	Catholic	White	Croatian	USA
79	430	M	Retired	Married	Orthodox	White	Slovenian	USA
80	435	F	Retired	Married	Catholic	White	Czech	USA
81	440	M	Retired	Married	Protestant	White	Slovak	USA
82	445	F	Retired	Married	Catholic	White	Hungarian	USA
83	450	M	Retired	Married	Orthodox	White	Romanian	USA
84	455	F	Retired	Married	Catholic	White	Bulgarian	USA
85	460	M	Retired	Married	Protestant	White	Serbian	USA
86	465	F	Retired	Married	Catholic	White	Croatian	USA
87	470	M	Retired	Married	Orthodox	White	Slovenian	USA
88	475	F	Retired	Married	Catholic	White	Czech	USA
89	480	M	Retired	Married	Protestant	White	Slovak	USA
90	485	F	Retired	Married	Catholic	White	Hungarian	USA
91	490	M	Retired	Married	Orthodox	White	Romanian	USA
92	495	F	Retired	Married	Catholic	White	Bulgarian	USA
93	500	M	Retired	Married	Protestant	White	Serbian	USA
94	505	F	Retired	Married	Catholic	White	Croatian	USA
95	510	M	Retired	Married	Orthodox	White	Slovenian	USA
96	515	F	Retired	Married	Catholic	White	Czech	USA
97	520	M	Retired	Married	Protestant	White	Slovak	USA
98	525	F	Retired	Married	Catholic	White	Hungarian	USA
99	530	M	Retired	Married	Orthodox	White	Romanian	USA
100	535	F	Retired	Married	Catholic	White	Bulgarian	USA

Table 2. Summary of data for the next 1000 cases.

Page 10

(Times given in LCT.)

Layer (in feet)	0200 (°C)	0500 (°C)	0800 (°C)	1100 (°C)	1300 (°C)	1600 (°C)	1900 (°C)	2200 (°C)
0-.5	2.71	2.30	.16	2.41	2.84	.77	5.60	2.26
.5-1.5	.62	.73	1.66	7.52	7.30	3.47	2.42	.55
1.5-3.0	.11	.17	2.07	7.81	7.25	3.43	.52	.37
3.0-6	-.14	-.12	1.57	5.84	5.20	2.41	-.37	-.06
6-12	-.28	-.30	.93	4.10	3.65	1.60	-.93	-.29
12-20	-.17	-.18	.76	3.15	3.23	1.31	-1.07	-.25
20-35	-.08	-.06	.60	2.08	2.24	.87	-.87	-.24
35-55	-.12	-.06	.54	2.13	1.66	.67	-.90	-.35
55-80	-.10	-.03	.47	1.08	1.19	.50	-.78	-.56
80-110	-.16	-.03	.25	.80	.93	.35	-.66	-.71
110-145	-.30	-.08	.27	.62	.75	.19	-.62	-.69
145-185	-.36	-.14	.35	.36	.45	.00	-.61	-.61
185-235	-.35	-.23	.30	.08	.22	-.15	-.62	-.57

Three-hourly Rate of Temperature-change Due to Carbon Dioxide

TABLE 4.

Table 3 gives the results obtained for net-outward radiation.

Table 4 gives the resultant rate of temperature-change for each slab of each sounding, computed using the results of Table 3 and equation (3.3).

3. Resultant Radiative Rate of Temperature-Change.

The temperature-change values of Tables 2 and 4 were added algebraically yielding a resultant radiative temperature-change for the slabs. Since these temperature-changes are to be compared with the observed temperature-change at the various boundaries it was necessary to adjust them to these boundaries. This was done by considering the radiative temperature-changes as existing at the midpoints of the slabs and then interpolating to the slab boundaries on log-log paper. These results are presented in Table 5, wherein all three-hourly rates have been reduced to half-hourly rates by dividing by 6.

(Times given in LCT)

Boundary (in feet)	0200 (°C)	0500 (°C)	0800 (°C)	1100 (°C)	1300 (°C)	1600 (°C)	1900 (°C)	2200 (°C)
.5	-.20	.24	-.40	2.21	2.77	1.42	2.02	.03
1.5	-.77	-.79	1.19	8.23	7.68	3.71	.35	-.58
3.0	-.71	-.69	1.49	6.19	6.34	2.93	-.32	-.51
6.0	-.47	-.47	1.40	4.25	3.72	1.98	-.42	-.53
12	-.30	-.33	.73	2.88	2.60	1.33	-.57	-.27
20	-.19	-.24	.47	1.87	2.06	.95	-.57	-.20
35	-.12	-.12	.34	1.28	1.25	.52	-.45	-.15
55	-.06	-.09	.31	.95	.86	.40	-.41	-.19
80	-.04	-.06	.23	.60	.59	.30	-.31	-.28
110	-.08	-.05	.13	.47	.50	.24	-.26	-.32
145	-.13	-.10	.14	.38	.41	.17	-.21	-.28
185	-.15	-.14	.17	.28	.30	.12	-.20	-.23
235	-.15	-.11	.10	.16	.20	.06	-.18	-.19

Half-hourly Rate of Temperature-change: Water Vapor + Carbon Dioxide

TABLE 5.

4. Rate of Change of Temperature Due to Molecular Conduction.

The flux due to molecular conduction was computed by the use of equation (3.8). The temperature, given in the observed data, for each level was used, hence the flux was considered as passing through the center of each layer. Consequently, the temperature-change computed from the value of the flux differences for two consecutive layers must be considered as being at the boundary between the two layers. This resulted in a rate of temperature-change at the boundary of each slab without the necessity of interpolation. The results obtained for rate of temperature-change due to molecular conduction are given in Table 6.

(Times given in LCT)

Boundary (in feet)	0200 (°C)	0500 (°C)	0800 (°C)	1100 (°C)	1300 (°C)	1600 (°C)	1900 (°C)	2200 (°C)
.5	-.90	-1.90	-1.60	7.20	8.0	4.10	-.57	-2.60
1.5	-.12	-.16	-.09	.57	.45	.17	-.27	0.0
3.0				.06	.07	.05	-.06	

Half-hourly Rate of Temperature-change Due to
Molecular Conduction

TABLE 6.

5. Rate of Change of Temperature Due to Eddy Conduction.

Those results follow immediately by the use of the observed $\frac{\partial T}{\partial x}$ and the values of Table 5 and 6 in equation (3.9). The values for the rate of temperature-change due to eddy conduction are given in Table 7.

...the ... of ...
 ...the ... of ...
 ...the ... of ...
 ...the ... of ...
 ...the ... of ...
 ...the ... of ...
 ...the ... of ...
 ...the ... of ...
 ...the ... of ...
 ...the ... of ...

Table 1. Results of the ...

Year	1990	1991	1992	1993	1994	1995	1996	1997
...
...
...

Table 2. Results of the ...

Table 3. Results of the ...

...the ... of ...
 ...the ... of ...
 ...the ... of ...
 ...the ... of ...
 ...the ... of ...

(Times given in LCT.)

Boundary (in feet)	0200 (°C)	0500 (°C)	0800 (°C)	1100 (°C)	1300 (°C)	1600 (°C)	1900 (°C)	2200 (°C)
.5	.80	1.66	1.60	-9.01	-10.37	-6.32	-1.05	-1.67
1.5	0.59	0.75	1.22	-7.60	-7.63	-4.48	-.02	0.18
3	0.21	0.49	0.47	-4.95	-5.91	-3.48	-.02	0.01
6	-0.23	0.17	0.50	-3.15	-3.62	-2.28	-0.28	-0.07
12	-0.30	0.03	0.97	-2.18	-2.20	-1.23	-0.33	-0.23
20	-0.31	0.04	1.43	-1.57	-2.36	-1.15	-0.03	-0.30
35	-0.48	-0.28	1.46	-0.78	-0.85	-0.52	0.15	-0.55
55	-0.34	-0.11	1.49	-0.45	-0.56	-0.30	0.31	-0.21
80	-0.06	-0.04	1.57	0.00	-0.59	-0.10	0.21	-0.22
110	0.28	0.05	0.47	-0.07	-0.10	-0.14	0.06	-0.28
145	0.03	0.30	1.46	0.02	-0.01	0.03	0.01	0.28
185	-0.05	0.14	1.33	0.02	0.20	0.08	-0.10	0.43
235	-0.35	0.12	1.30	.04	0.10	0.04	0.08	.39

Half-hourly Temperature-change Due to
Eddy Conduction

TABLE 7.

V. RESULTS AND CONCLUSIONS

1. Method of Computation of the Coefficient of Eddy Conductivity.

As indicated in Chapter III, Section 5, it was decided to determine for all soundings evaluated a first value of K from the theory of turbulent transfer of momentum. For this purpose it was necessary to make use of observed winds in order to evaluate $\frac{\partial \bar{u}}{\partial Z}$ for use in equation (3.12). Two winds were given consistently in the data which were always within the surface layer, one at 12 feet and one at 41 feet. For each of the eight soundings studied, these two values of the wind were plotted against $\log Z$ on semi-log paper, and a straight line joining the two points was drawn. The value of $\frac{\partial \bar{u}}{\partial Z}$ in the vicinity of 16 feet was then read off as being the value $\frac{\Delta u}{\Delta Z}$ corresponding to a height increment of 100 centimeters at 16 feet. The reasons for choosing the 16 foot level as the standard reference level are two-fold:

(a) The level had to be within the lowest levels for which wind data are available.

(b) The level had to be within the lowest slab consistent with (a) for which lapse rate data is available. This is necessary since, in equation (3.13), the mixing length, l , involves $\frac{\partial \theta}{\partial Z} \div \left(\frac{\partial T}{\partial Z} + \gamma_d \right)$.

In satisfying requirement (b), it was necessary to use the slab 12-20 feet, which was considered to define $\frac{\partial \theta}{\partial Z}$ at 16 feet.

In several cases however, it was necessary to shift to the level 23.5 feet. This necessity arose when an obviously inconsistent lapse rate was indicated in the layer 12-20 feet. This shifting to the level 23.5 feet

Let X and Y be random variables defined on the same probability space. The joint probability distribution of X and Y is a function $p(x, y)$ defined on the set $\mathcal{X} \times \mathcal{Y}$ of possible values of X and Y . The joint distribution must satisfy the following conditions:

- (1) $p(x, y) \geq 0$ for all $(x, y) \in \mathcal{X} \times \mathcal{Y}$.
- (2) $\sum_{(x, y) \in \mathcal{X} \times \mathcal{Y}} p(x, y) = 1$.

The marginal probability distributions of X and Y are defined by

$$p_X(x) = \sum_{y \in \mathcal{Y}} p(x, y) \quad \text{and} \quad p_Y(y) = \sum_{x \in \mathcal{X}} p(x, y).$$

The joint distribution $p(x, y)$ is said to be independent if

$$p(x, y) = p_X(x) p_Y(y) \quad \text{for all } (x, y) \in \mathcal{X} \times \mathcal{Y}.$$

The joint distribution $p(x, y)$ is said to be bivariate normal if it has the form

$$p(x, y) = \frac{1}{2\pi\sigma_1\sigma_2\sqrt{1-\rho^2}} \exp\left\{-\frac{1}{2(1-\rho^2)}\left[\frac{x-\mu_1}{\sigma_1} - \rho\frac{y-\mu_2}{\sigma_2}\right]^2 - \frac{1}{2(1-\rho^2)}\left[\frac{y-\mu_2}{\sigma_2} - \rho\frac{x-\mu_1}{\sigma_1}\right]^2\right\}$$

where $\mu_1, \mu_2, \sigma_1, \sigma_2$ are real numbers and ρ is a real number with $|\rho| < 1$.

PROBLEM SET 1

1. Let X and Y be random variables with joint probability distribution

$$p(x, y) = \frac{1}{10} \begin{cases} 1 & \text{if } (x, y) = (1, 1), (1, 2), (2, 1), (2, 2), \\ & (3, 1), (3, 2), (4, 1), (4, 2) \\ 0 & \text{otherwise} \end{cases}$$

(a) Find the marginal probability distributions of X and Y .

(b) Find the conditional probability distributions of X and Y given the other variable.

(c) Find the covariance and correlation coefficient of X and Y .

$$\text{Answer: (a) } p_X(x) = \frac{1}{5} \text{ for } x = 1, 2, 3, 4; \quad p_Y(y) = \frac{1}{5} \text{ for } y = 1, 2.$$

(b) $p_{X|Y}(x|y) = \frac{1}{4}$ for $x = 1, 2, 3, 4$ and $y = 1, 2$.

(c) $\text{Cov}(X, Y) = 0$, $\rho = 0$.

2. Let X and Y be random variables with joint probability distribution

amounted to dealing with the over-all lapse rate in the layer 12-35 feet, which then gave $\frac{\partial \theta}{\partial Z}$ at 23.5 feet.

In order to evaluate the mixing length, l (the remaining ^{factor} term of equation (3.12)) at the standard level, a knowledge of the corresponding value l_a , the mixing length in an isotropic atmosphere, is necessary. According to Lettau [9] isotropic or adiabatic turbulence is most nearly realized around sunset or sunrise. Thus, in order to derive the adiabatic velocity-profile for the 24-hour period under investigation, an average of three half-hourly wind-speed reports at both sunrise and sunset was obtained. Then, plotting mean wind-speed against $\log Z$ on semi-log paper for the two values of Z a straight line was obtained, Figure 3, which according to Lettau should represent the wind profile for Manor, Texas under adiabatic conditions for 27-28 September 1948. The straight line obtained apparently does represent a close approximation to the true adiabatic atmosphere, since Figure 3 indicates a roughness parameter $Z_0 = 2$ cms, which checks rather well with values quoted by Stewart [1] for fallow fields. Knowing the value of the roughness parameter permits the computation of l_a from equation (3.13).

The value of $\frac{\partial u_a}{\partial Z}$ at 16 feet was then read directly off the velocity profile of Figure 3. Since 16 feet \approx 490 cms this can be done quite simply by reading off the wind-speed differences between 600 and 400 cms and dividing by 200 cms. This calculation leads to $.15 \text{ sec}^{-1}$, a value which may be checked mathematically using the theoretical equation of the straight line of Figure 3. This is done below.

... and $\frac{1}{2}$ is $\frac{28}{32}$, ...

... and $\frac{1}{2}$ is $\frac{28}{32}$, ...

... and $\frac{1}{2}$ is $\frac{28}{32}$, ...

... and $\frac{1}{2}$ is $\frac{28}{32}$, ...

... and $\frac{1}{2}$ is $\frac{28}{32}$, ...

... and $\frac{1}{2}$ is $\frac{28}{32}$, ...

... and $\frac{1}{2}$ is $\frac{28}{32}$, ...

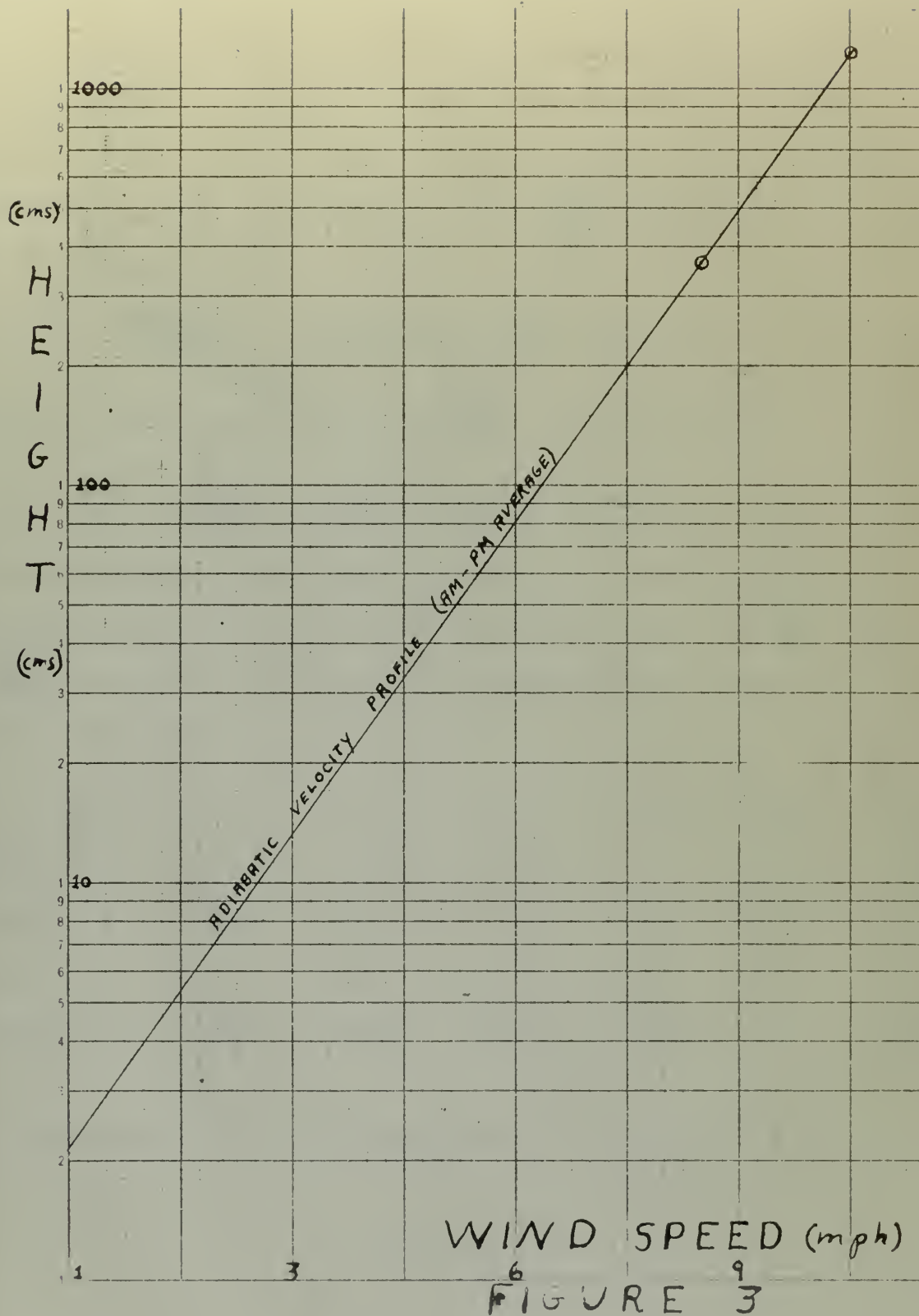
... and $\frac{1}{2}$ is $\frac{28}{32}$, ...

... and $\frac{1}{2}$ is $\frac{28}{32}$, ...

... and $\frac{1}{2}$ is $\frac{28}{32}$, ...

... and $\frac{1}{2}$ is $\frac{28}{32}$, ...

... and $\frac{1}{2}$ is $\frac{28}{32}$, ...



Adiabatic Velocity Profile

Figure 3.

The equation of the wind profile line of Figure 3 can be written as in (3.15). Using the mean value of U_a at the 12 foot level (366 cms), $k = .45$, $Z_0 = 2$ cms, $U_a = 3.8$ mps, we obtain $\sqrt{\frac{\tau}{\rho}} = 32.8$ cm sec⁻¹. Then from equation (16),

$$\left(\frac{\partial u_a}{\partial Z}\right)_{Z=16ft} = \frac{1}{.45}(32.8) \left(\frac{1}{490}\right) = .15 \text{ sec}^{-1}.$$

Similarly at 23.5 feet the value of $\frac{\partial u_a}{\partial Z}$ was found to be:

$$\frac{\partial u_a}{\partial Z} = \frac{1}{.45}(32.8) \frac{1}{718} = .10 \text{ sec}^{-1}.$$

At these two levels $l_a = 220$ and 323 cms, respectively. Values of K at the reference level may now be determined once the values of $\frac{\partial \theta}{\partial Z}$, θ'_c , $\frac{\partial \bar{u}}{\partial Z}$ are known. These results are tabulated below in Table 8 for the various times of day:

	0200*	0500*	1100*	1300	1600	1900	2200
$\frac{\partial \theta}{\partial Z}$ °C/cm	.00067	.00038	-.00075	-.0028	-.00061	.00092	.00092
θ'_c °C/cm	.0030	.0030	.0031	.0066	.0030	.0066	.0065
$\frac{\partial \bar{u}}{\partial Z}$ sec ⁻¹	.183	.34	.215	.438	.222	.214	.438
K cm ² sec ⁻¹	13,000	28,000	40,900	63,800	38,000	8,000	16,000

Computation Values for Determination of K at Reference Level

TABLE 8.

the system is in a state of equilibrium, the total energy is constant.

Let us consider a system of particles, each of mass m , moving with velocity v .

$$K = \frac{1}{2}mv^2 = \frac{1}{2}m \left(\frac{dx}{dt} \right)^2 = \frac{1}{2}m \frac{dx^2}{dt^2} = \frac{1}{2}m \frac{d^2x}{dt^2} \cdot dt = \frac{1}{2}m \frac{d^2x}{dt^2} \cdot dt$$

where K is the kinetic energy.

$$K = \frac{1}{2}mv^2 = \frac{1}{2}m \left(\frac{dx}{dt} \right)^2 = \frac{1}{2}m \frac{dx^2}{dt^2} = \frac{1}{2}m \frac{d^2x}{dt^2} \cdot dt = \frac{1}{2}m \frac{d^2x}{dt^2} \cdot dt$$

$$K = \frac{1}{2}mv^2 = \frac{1}{2}m \left(\frac{dx}{dt} \right)^2 = \frac{1}{2}m \frac{dx^2}{dt^2} = \frac{1}{2}m \frac{d^2x}{dt^2} \cdot dt = \frac{1}{2}m \frac{d^2x}{dt^2} \cdot dt$$

$$K = \frac{1}{2}mv^2 = \frac{1}{2}m \left(\frac{dx}{dt} \right)^2 = \frac{1}{2}m \frac{dx^2}{dt^2} = \frac{1}{2}m \frac{d^2x}{dt^2} \cdot dt = \frac{1}{2}m \frac{d^2x}{dt^2} \cdot dt$$

Let us consider a system of particles, each of mass m , moving with velocity v .

$$K = \frac{1}{2}mv^2 = \frac{1}{2}m \left(\frac{dx}{dt} \right)^2 = \frac{1}{2}m \frac{dx^2}{dt^2} = \frac{1}{2}m \frac{d^2x}{dt^2} \cdot dt = \frac{1}{2}m \frac{d^2x}{dt^2} \cdot dt$$

$$K = \frac{1}{2}mv^2 = \frac{1}{2}m \left(\frac{dx}{dt} \right)^2 = \frac{1}{2}m \frac{dx^2}{dt^2} = \frac{1}{2}m \frac{d^2x}{dt^2} \cdot dt = \frac{1}{2}m \frac{d^2x}{dt^2} \cdot dt$$

where K is the kinetic energy.

CC	CC	CC	CC	CC	CC	CC	CC
1000	1000	1000	1000	1000	1000	1000	1000
1000	1000	1000	1000	1000	1000	1000	1000
1000	1000	1000	1000	1000	1000	1000	1000
1000	1000	1000	1000	1000	1000	1000	1000

Let us consider a system of particles, each of mass m , moving with velocity v .

$$K = \frac{1}{2}mv^2$$

In Table 8, the * alongside the time indicates that the reference level was taken at 23.5 feet due to the non-representative lapse rates between 12 and 20 feet. The 0800 values of K were not computed since many of the slabs had either non-representative or dry adiabatic* lapse rates so that the heat transport equations (3.11) yield no solutions.

For all soundings, other than the 0800 sounding, it was possible to obtain solutions of equations (3.11) using the values of K of Table 8 as a starting point. The values of K for 0200, 0500, 1100, 1300, 1600, 1900 and 2200 LCT at the indicated elevations are listed in Table 9, and shown graphically in Plate I. In Table 9 the occurrence of blank spaces indicates the existence of a non-representative lapse rate in the slab having the indicated height as its midpoint. It was therefore necessary to consolidate adjacent slabs, obtaining a value of K corresponding to the new midpoint, as discussed earlier in Section 1 of this chapter.

*Actually, isothermal lapse rates were not significantly different from the dry adiabatic for many of the layers under study, when the gust error of $\pm .2^{\circ}\text{C}$ is considered.

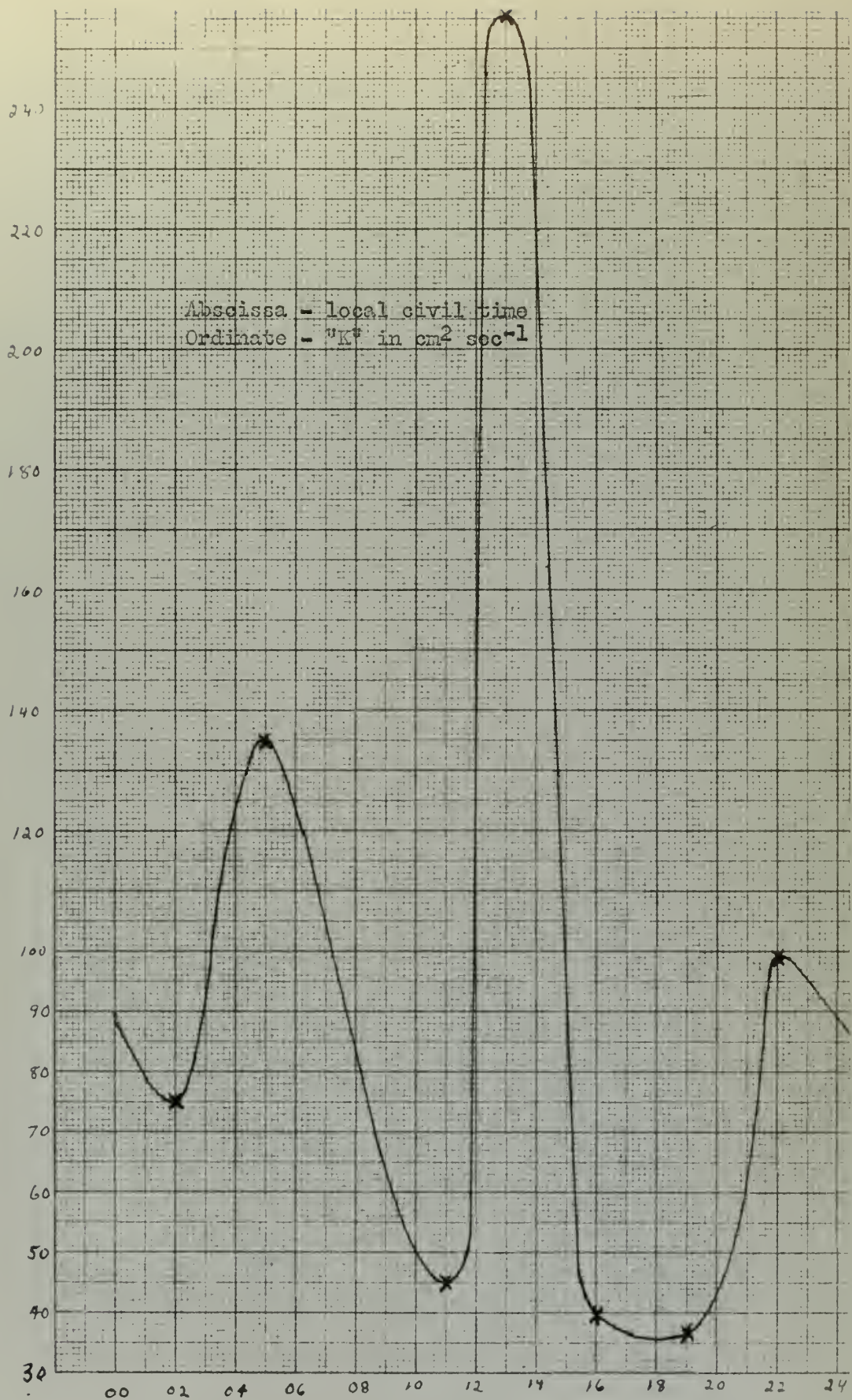
(Times given in LCT.)

Level (feet)	0200 $K(10)^3$	0500 $K(10)^3$	1100 $K(10)^3$	1300 $K(10)^3$	1600 $K(10)^3$	1900 $K(10)^3$	2200 $K(10)^3$
.25	.075	.14	.045	.26	.04	.036	.099
1.0	.51	.68	.50	3.7	.66	.16	
2.25	1.9	3.0	2.4	16.4	1.7	.41	2.3
4.5	1.5	2.4	5.8	180.		.73	2.3
7.5					15.		
9.0	4.9	5.9	20.	48.		1.3	6.7
16.0				64.	38.	8.0	16.
23.5	13.	28.	41.				
27.5				500.	63.	5.1	9.2
45.0	11.	23.	480.	1700.	35.	8.0	11.
67.5	17.	28.		300.	130.	32.	9.0
82.5			120.				
95.0	8.	21.				73.	20.
127.5	10.	18.	350.			25.	530.
165.0	17.	20.				28.	840.
210.0	17.	82.				210.	920.
261.5	18.	87.				190.	1500.

The Coefficient of Eddy Conduction, K , ($\text{cm}^2 \text{ sec}^{-1}$)

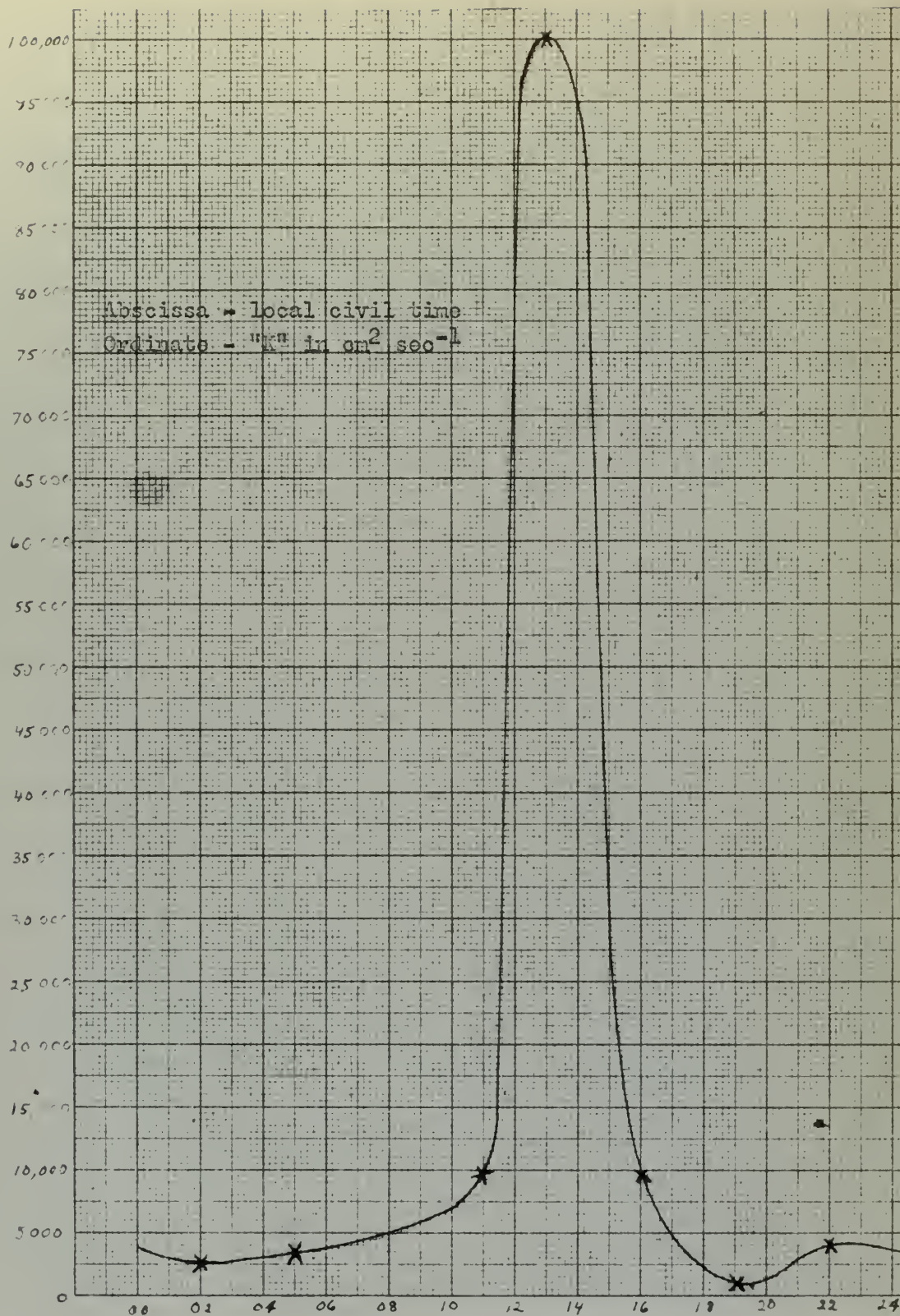
TABLE 9.

In order to show more clearly the variations of K with both height and time, graphs of K at fixed elevations were drawn showing the time-variation of K at these elevations. The fixed elevations used are 3 inches, 6, 30, 60 and 125 feet and the results are shown in Figures 4, 5, 6, 7, and 8.



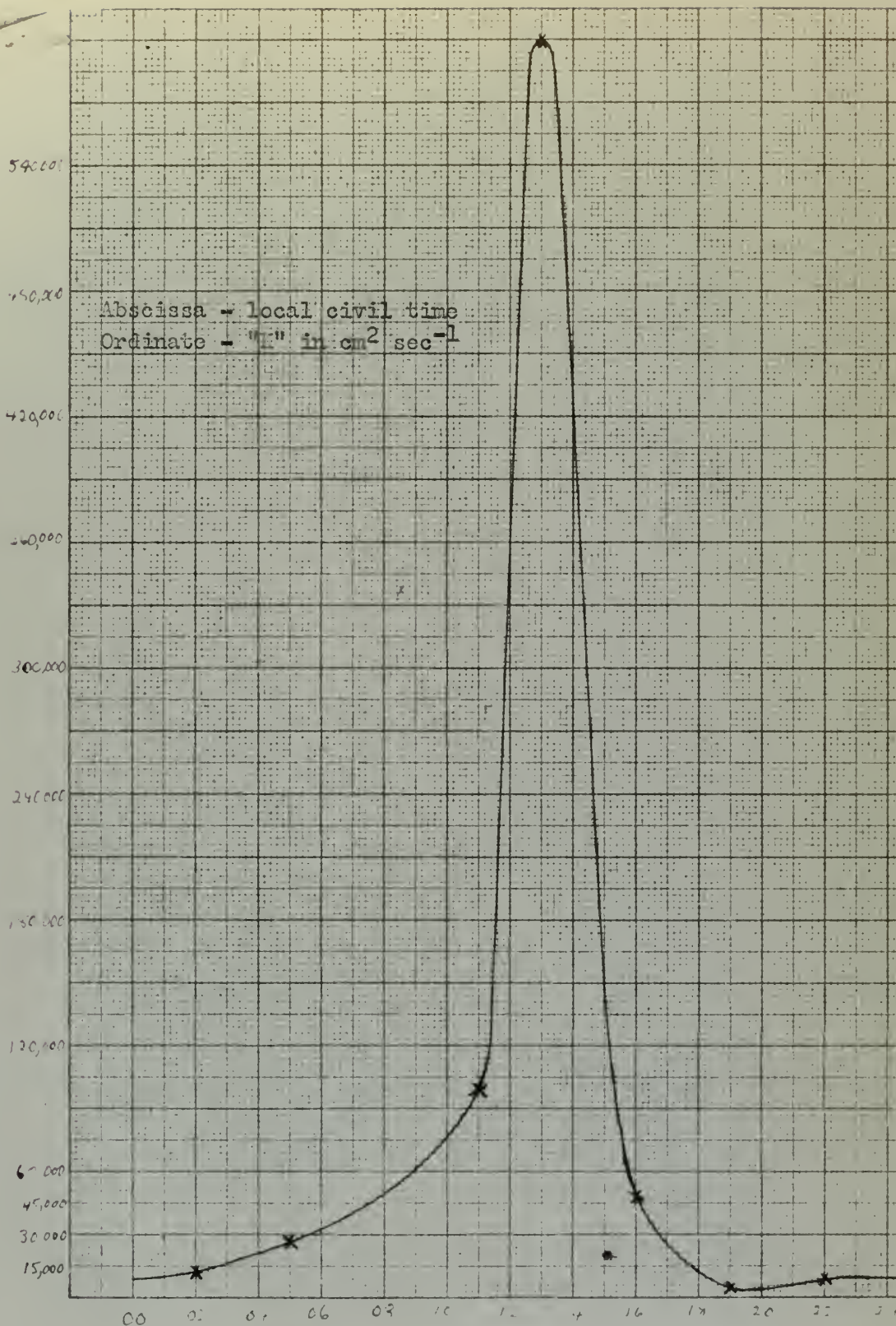
Diurnal Variation of "K" at .25 Feet

Figure 4.



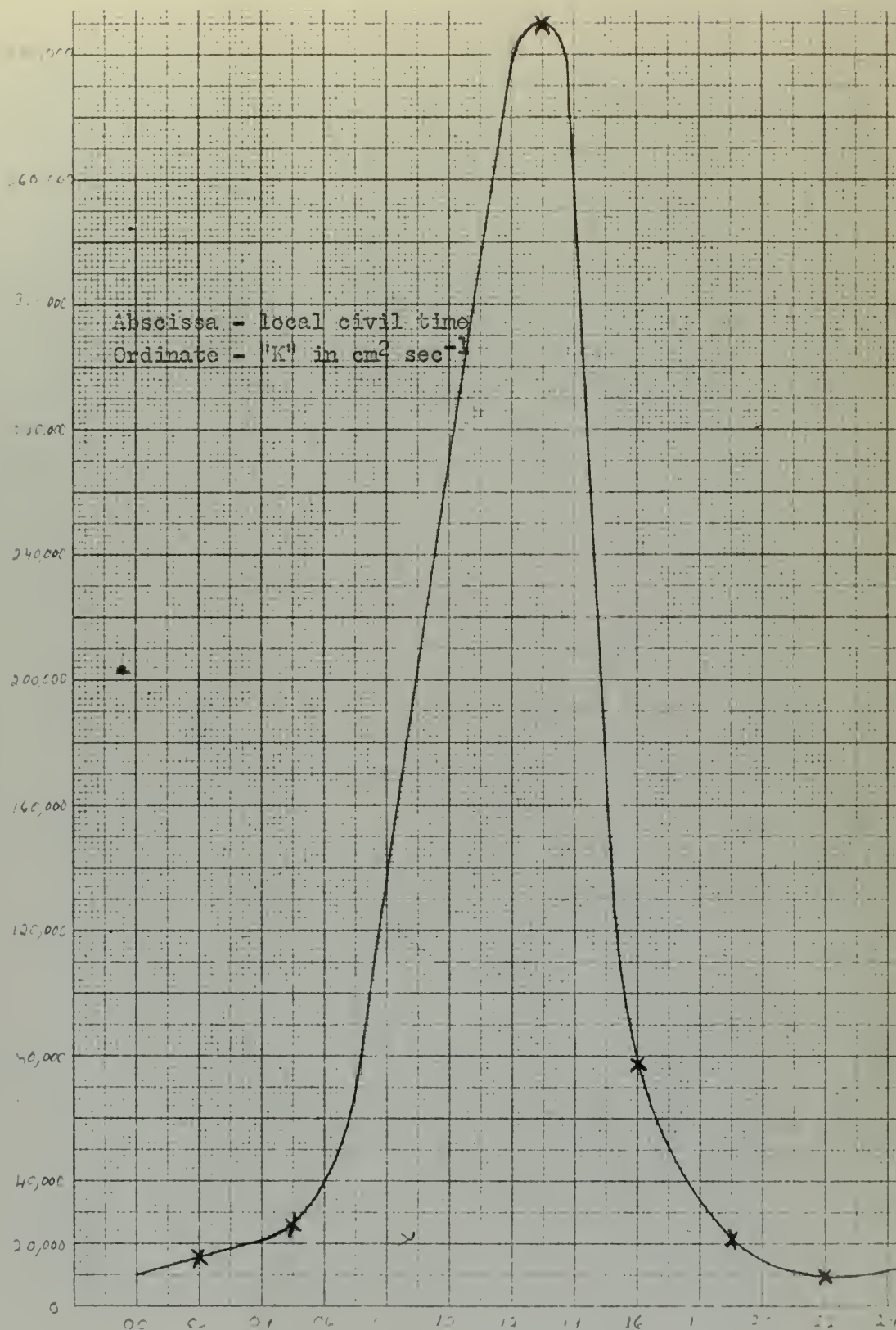
Diurnal Variation of "K" at 6 Feet

Figure 5.



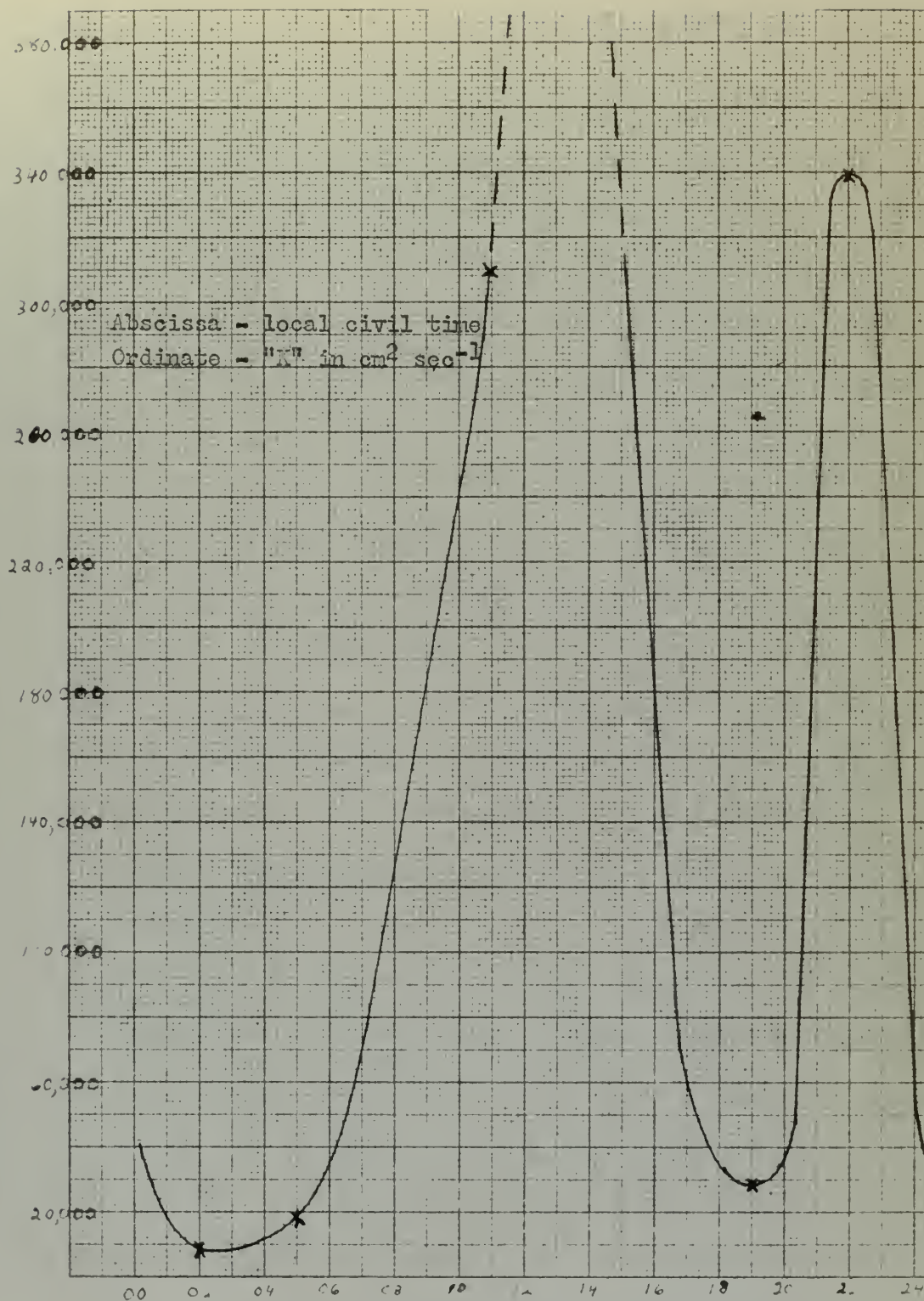
Diurnal Variation of "K" at 30 Feet

Figure 6.



Diurnal Variation of "K" at 60 Feet

Figure 7.



Diurnal Variation of "K" at 125 Feet

Figure 8.

2. Discussion of Results.

Lettau [9] has defined the surface layer essentially as the layer in which the turbulent time-rate of change of a property is negligible in comparison with its turbulent flux. In the solution of equations (3.11) for the various levels, it is evident that the value of the lapse rates become exceedingly critical as the value of the lapse rate approaches the dry adiabatic γ_d . For, if the maximum gust error ± 0.2 °C occurred in opposite senses at adjacent levels, it would cause an error in observation of the lapse rate by several times γ_d , depending upon the layer thickness. Thus it follows that the most representative values of K may be expected where the lapse rate γ is largest compared to γ_d and especially where it is of the order of 50-100 (or more) times γ_d . In order to emphasize this dependence upon lapse rate, let us consider the values of the lapse rate in the various layers for the 0200 and 1300 LCT soundings. These are shown in Table 10. In this table, the abbreviation "n.r." indicates a non-representative lapse rate; therefore, necessitating a consolidation of the two adjacent layers.

Notice, from Table 10, that at 1300 LCT the lapse rates were strongly super-adiabatic near the ground but not significantly different from the dry adiabatic above 80 feet. At 0200 LCT the lapse rates were more nearly uniform than at 1300 LCT. A comparison shows that the 1300 LCT lapse rates were numerically greater than those for 0200 LCT between the surface and 6 feet, but, above 6 feet, the early morning lapse rates in general exceed those of mid-day. For purposes of comparison, the value of the dry adiabatic lapse rate is $\gamma_d = .98 \times 10^{-4}$ °C per cm.

THEORY OF THE [1] THEORY OF THE

THEORY OF THE [2] THEORY OF THE

THEORY OF THE [3] THEORY OF THE

THEORY OF THE [4] THEORY OF THE

THEORY OF THE [5] THEORY OF THE

THEORY OF THE [6] THEORY OF THE

THEORY OF THE [7] THEORY OF THE

THEORY OF THE [8] THEORY OF THE

THEORY OF THE [9] THEORY OF THE

THEORY OF THE [10] THEORY OF THE

THEORY OF THE [11] THEORY OF THE

THEORY OF THE [12] THEORY OF THE

THEORY OF THE [13] THEORY OF THE

THEORY OF THE [14] THEORY OF THE

THEORY OF THE [15] THEORY OF THE

THEORY OF THE [16] THEORY OF THE

THEORY OF THE [17] THEORY OF THE

THEORY OF THE [18] THEORY OF THE

THEORY OF THE [19] THEORY OF THE

THEORY OF THE [20] THEORY OF THE

THEORY OF THE [21] THEORY OF THE

THEORY OF THE [22] THEORY OF THE

THEORY OF THE [23] THEORY OF THE

THEORY OF THE [24] THEORY OF THE

THEORY OF THE [25] THEORY OF THE

Layer (feet)	Lapse Rate ($^{\circ}\text{C}/\text{cm}$) $\times 10^{-4}$	
	0200 LCT	1300 LCT
0-.5	-1.1×10^3	7.1×10^3
.5-1.5	-1.6×10^2	4.9×10^2
1.5-3	-44	110
3-6	-55	11
6-12	-16	38
12-20	n.r.	29
20-35	-5.7	13
35-55	n.r.	4.4
55-80	-6.6	4.9
80-110	-3.9	1.3
110-145	-9.8	8.0
145-185	-7.5	isothermal
185-235	-4.1	"
	-3.9	"

Values of Lapse Rates at 0200 and 1300 LCT

TABLE 10.

In general, it was found that when γ was significantly different from γ_d , the turbulent rate of change term of equations (3.11) was completely negligible. Due to the inability to smooth out the turbulent fluctuations of temperature, the definition of the surface layer in this study is the layer in which the lapse rate is significantly different from dry adiabatic, both the gust and instrumental errors being considered. Thus the surface layer at 1300 LCT extends to about 80 feet, but at 0200 LCT extends to at least 235 feet. This is evident from the values of Table 10. It must be realized that a negative value of this lapse rate is more significantly different from γ_d than a corresponding positive value of the lapse rate. Then, for all practical purposes, equation (3.11) within the surface layer reduces to:

$$K_1 \left(\frac{\partial T}{\partial Z} + \gamma_d \right)_1 - K_2 \left(\frac{\partial T}{\partial Z} + \gamma_d \right)_2 = 0, \quad (5.1)$$

where subscripts 1 and 2 refer to a lower and upper level, respectively.

Let us consider the actual values of K shown in Plate I in which the value of K is plotted on a log-log scale against the height of the midpoint of the slab to which the value of K corresponds. It is noted that, for any sounding, the first three points in order of ascending height are very close to a straight line, there being some deviation from the straight line relationship as the fourth, fifth, etc., points are considered. This deviation, commencing with the fourth point, is due mainly to two factors:

- (1) Decreasing, therefore less representative, values of the lapse rate.
- (2) The change in temperature elements above the three foot level; there being non-aerated resistors below and aerated resistors above.

Therefore, it was considered permissible to fit the best line to each sounding in Plate I up to the maximum height for which K and Z both increase together. The line of best fit for each sounding was drawn in accordance with the following principles:

- (a) Through the first point.
- (b) Through as many additional points as possible.
- (c) Separating approximately equal numbers of points.

The slopes and heights to which these lines may be considered representative are shown in Table 11 for each sounding.

Sounding (Time in LCT)	Slope of line, m	Maximum height of linear distribution (feet)	Values of K_1 in equation (5.3) ($\text{cm}^2\text{-m sec}^{-1}$)
0200	1.14	23.5	365
0500	1.17	23.5	506
1100	1.79	45.0	536
1300	1.69	45.0	2660
1600	1.70	23.5	410
1900	1.05	45.0	155
2200	1.23	16.0	544

Slopes of Log K Against Log Z for the Lines of Plate I

TABLE 11.

There is a tendency for the lines for the 1900 and 2200 LCT soundings to continue to be representative up to 235 feet. However, for the 0200 and 0500 LCT soundings beyond 23.5 feet, the points fall well below the line. This suggests the possibility of fitting a curve other than a straight line (perhaps a parabola) in the early morning hours; however, this idea was not pursued further.

If we write the equation of any straight line of Plate I in the form

$$\log K = m(\log Z) + b, \quad (5.2)$$

where m is the measured slope (see Table 11) of the line, we obtain upon raising to powers of 10, the equation

$$K = 10^b Z^m = K_1 Z^m. \quad (5.3)$$

Since each line passes through the point corresponding to $Z = 1/4$ foot, the value of K_1 for each sounding may be assigned by setting $Z = 1/4$ and K to its appropriate value. The values of K_1 for each sounding are shown in the last column of Table 11. Equation (5.3), with the appropriate values of K_1 and m , represent the distribution of K with respect to height for the various times of day and up to the heights indicated in Table 11. This is the chief empirical result of this study.

Finally, we shall state the conclusions resulting from the foregoing analysis and from Figures 4 through 8. These conclusions are:

- (1) The average mid-day value of m is 1.73.
- (2) The average value of m near midnight is 1.18.
- (3) The value of m seems to approach unity at sunset.
- (4) The exponent m appears to be a function of stability.

(5) The maximum value of K, level for level up to 60 feet, appears to occur at about 1300 LCT, at about the time of the maximum surface temperature. The power law satisfied by K at this time of day is

$$K = 2660 Z^{1.69},$$

where Z is the height in feet.

(6) The minimum value for K, level for level up to 60 feet, appears to occur about 1900 LCT, with a very slow rate of increase during the night.

(7) From Figure 8 at 125 feet there appears to be a second pronounced diurnal maximum of K at 2200 LCT. This appears to be due to the diurnal variation in the height of the surface layer. According to Lettau [8], the surface layer is characterized by increasing values of K with height, with decreasing values of K occurring above this layer. If, during the daylight hours the 125 foot level is above the surface layer, but passes into it at about 2200 LCT, the large increase in the value of K at 125 feet appears to be reasonable.

BIBLIOGRAPHY

1. Berry, F. A., Jr., E. Bollay, and N. R. Beers. Handbook of Meteorology, New York, McGraw-Hill, 1945.
2. Brunt, D. Radiation in the Atmosphere, Quarterly Journal Royal Meteorological Society, 66: 35-40, 1940.
3. Callendar, C. S. Infra-red Absorption by Carbon Dioxide, with Special Reference to Atmospheric Radiation. Quarterly Journal Royal Meteorological Society, 67: 263-275, 1941.
4. Dennison, D. M., N. Ginsberg and L. R. Weber. Physical Review, 52: 160-174, 1937.
5. Elsasser, W. . Heat Transfer by Infra-red Radiation in the Atmosphere, Harvard University, Blue Hill Meteorological Observatory, Milton, Mass. 1942. (Harvard Meteorological Studies No. 6).
6. Gerhardt, J. R., K. H. Jehn, W. R. Guild, and R. C. Staley. Micrometeorological Research Data, Vol. II. Electrical Engineering Research Laboratory, The University of Texas, (Report No. 29). 1 June 1949.
7. Haurwitz, Bernard. Dynamic Meteorology. New York, McGraw-Hill, 1941.
8. Lettau, H. Atmosphärische Turbulenz, Leipzig, 1939.
9. Lettau, H. Isotropic and Non-isotropic Turbulence in the Atmospheric Surface Layer. Geophysical Research Papers No. 1; Base Directorate for Geophysical Research, Air Force Cambridge Research Laboratories, Cambridge, Massachusetts. December 1949.
10. Panofsky, H. A. Radiative Cooling in the Lowest Layers of an Atmosphere Warmer Than the Ground. The Journal of Meteorology. 4: 35-37, February 1947.
11. Petterssen, S. and W. C. Swinbank. On The Application of The Richardson Criterion to Large-scale Turbulence in the Free Atmosphere. Quarterly Journal of the Royal Meteorological Society. 73: 335-345, July-October 1947.
12. Sverdrup, H. U. Geophysiske Publ. Vol. 11, 1936.

1,000,000
900,000
800,000

600,000

400,000

200,000

100,000

80,000

60,000

40,000

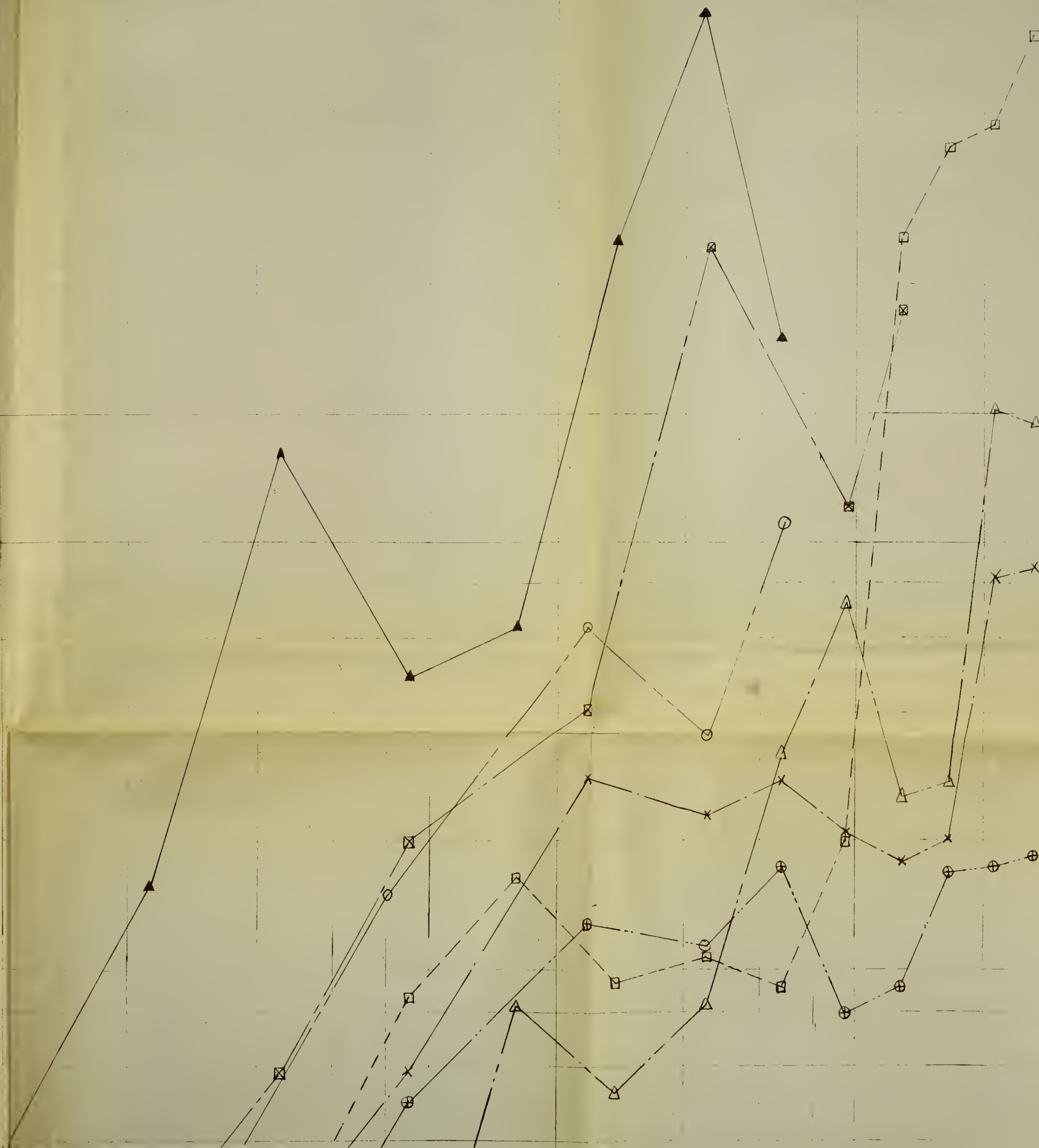
20,000

10,000

8,000

6,000

K



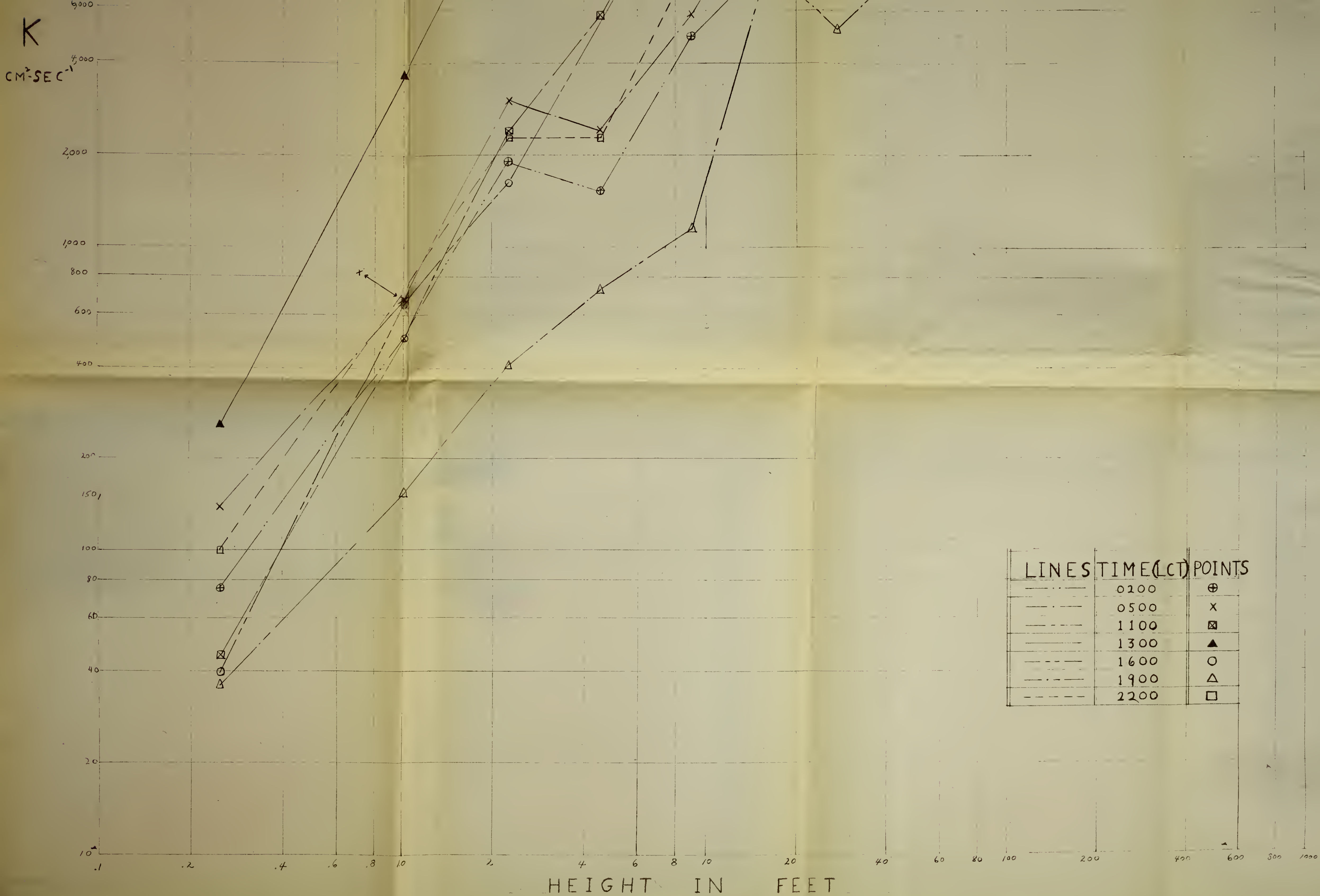


PLATE I - VARIATION OF K WITH HEIGHT



JL 258

Thesis

C748

Cooley

Determination of the
diurnal variation of
eddy conductivity near
the earth's surface

JL 258

INTERLIB

Quartermaster

13128

INTERLIB

Quartermaster
Process. Eng.
Cent. Nat. Lab.
Mass.

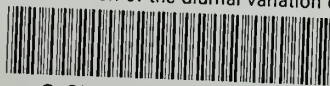
JA.2160

9469

Th
C
D
a
e

thesC748

Determination of the diurnal variation o



3 2768 002 09395 7

DUDLEY KNOX LIBRARY